



# Design and Production of a New Smaller Diameter Axial Bearing Subjected to High Wear Loads

Submitted to the Graduate School of Natural and Applied Sciences  
in partial fulfillment of the requirements for the degree of

Master of Science

in Mechanical Engineering

by

Sinan Dayı

ORCID



May, 2021

This is to certify that we have read the thesis **Design and Production of a New Smaller Diameter Axial Bearing Subjected to High Wear Loads** submitted by **Sinan Dayı**, and it has been judged to be successful, in scope and in quality, at the defense exam and accepted by our jury as a MASTER'S THESIS.

**APPROVED BY:**

**Advisor:** **Prof. Dr. Mehmet ÇEVİK** .....  
İzmir Kâtip Çelebi University

**Committee Members:**

**Assist. Prof. Dr. Ebubekir Atan** .....  
İzmir Kâtip Çelebi University

**Assist. Prof. Dr. Saim Kural** .....  
Manisa Celal Bayar University

**Date of Defense: May 05, 2021**

# Declaration of Authorship

I, **Sinan Dayı**, declare that this thesis titled **Design and Production of a New Smaller Diameter Axial Bearing Subjected to High Wear Loads** and the work presented in it are my own. I confirm that:

- This work was done wholly or mainly while in candidature for the Master's degree at this university.
- Where any part of this thesis has previously been submitted for a degree or any other qualification at this university or any other institution, this has been clearly stated.
- Where I have consulted the published work of others, this is always clearly attributed.
- Where I have quoted from the work of others, the source is always given. This thesis is entirely my own work, with the exception of such quotations.
- I have acknowledged all major sources of assistance.
- Where the thesis is based on work done by myself jointly with others, I have made clear exactly what was done by others and what I have contributed myself.

Signature:

---

Date: 05.05.2021

---

# Design and Production of a New Smaller Diameter Axial Bearing Subjected to High Wear Loads

## Abstract

In the steering system of a passenger car, one of the essential components is the tie rod, and the sub-assembly component is the inner tie rod, which is subject to static and dynamic bearing loads. These bearing loads are the key points to ensure the inner tie rod's performance and total lifetime. A significant drop in the inner tie rod's performance can cause uncomfortable driving conditions and noise during driving. Most of the designs are developed over-safe with bigger ball sizes to fulfill the defined requirements. On the other hand, over-safe design can cause higher prices.

In this study, a new small diameter axial bearing system is developed subjected to high wear loads on the inner tie rod. Three design parameters are considered: press force, tempering method, and tempering temperature. A smaller ball diameter design is created during the development phase. After the manufacturing, the inner tie rods are tested concerning the wear test and setting behaviour under the maximum loading test. Results have been compared with a bigger ball size design. By changing the production and assembly parameters, optimum assembly conditions have been defined. Functional measurements before and after testing have validated the new smaller ball diameter design for serial usage.

**Keywords:** Steering system, inner tie rod, axial bearing

# Yüksek Aşınma Yüklerine Maruz Yeni Bir Küçük Çaplı Eksenel Yatak Tasarımı ve İmalatı

## ÖZ

Bir binek otomobilin direksiyon sisteminde en önemli bileşenlerden biri rot kolu ve alt montaj bileşeni olarak statik ve dinamik yatak yüklerine maruz kalan rot milidir. Bu yatak yükleri, rot milinin performansını ve toplam ömrünü sağlamak için kilit noktadır. Rot milinin eksenel yatak performansında önemli bir düşüş, rahatsız edici sürüş koşullarına ve ayrıca sürüş sırasında gürültüye neden olabilir. Tasarımların çoğu, tanımlanan gereksinimlerin karşılanmasını sağlamak için daha büyük küre boyutuyla geliştirilir. Öte yandan, aşırı güvenli tasarım daha yüksek fiyatlara neden olabilir.

Bu çalışmada, rot milinde yüksek aşınma yüklerine maruz kalan yeni bir küçük çaplı eksenel yatak sistemi geliştirilmiştir. Üç tasarım parametresi kullanılmıştır, bunlar; kapatma kuvveti, temperleme tipi ve temperleme sıcaklığıdır. Geliştirme aşamasında daha küçük küre çapı tasarımı oluşturulmuş ve üretilmiştir. İmalattan sonra, rot milinin eksenel yatağının aşınma testi ve maksimum yükleme testi altında davranışı açısından testler yapılmıştır. Sonuçlar daha büyük küre çapıyla üretilen tasarımla karşılaştırılmıştır. Üretim ve montaj parametreleri değiştirilerek optimum montaj koşulları tanımlanmıştır. Test öncesi ve sonrası fonksiyonel ölçümler, seri kullanım için yeni daha küçük küre çaplı tasarımı doğrulamıştır.

**Anahtar kelimeler:** Direksiyon sistemi, rot mili, eksenel yatak



*To my family...*

# Acknowledgment

I would like to thank to my supervisor, Prof. Dr. Mehmet EVİK, for providing guidance and feedback throughout this project. Thanks to ZF Lemfölder Aks Modülleri San. ve Tic. A.Ş. for providing production and testing possibilities during the project. Thanks to my colleagues Hasan Ender Erdoğan, Buğra Yiğit Çetin for their support.

# Table of Contents

Declaration of Authorship .....	ii
Abstract .....	iii
Öz .....	iv
Acknowledgment .....	vi
List of Figures .....	ix
List of Tables.....	xi
List of Abbreviations.....	xii
List of Symbols.....	xiii
<b>1 Introduction.....</b>	<b>1</b>
1.1 Steering System.....	2
1.1.1 Mechanical steering systems.....	4
1.2 Steering Tie Rods .....	7
1.2.1 Inner Tie Rod (ITR) .....	12
1.3 Literature Review on Tie Rods.....	15
<b>2 Bearing System.....</b>	<b>17</b>
2.1 Wear Mechanism in Bearing Systems.....	17
2.2 The wear system .....	18
2.2.1 Properties of polyoxymethylene (POM) .....	20
2.3 Literature Review on Bearing Systems .....	22
<b>3 Material and Method .....</b>	<b>26</b>
3.1 Material.....	26
3.1.1 Assembly.....	27
3.2.1 Tempering .....	29
3.2 Method.....	32
3.2.1 Functional measurements.....	38



3.2.2 Setting Test.....	44
3.2.3 Wear Test .....	47
<b>4 Results and Discussions .....</b>	<b>50</b>
4.1 Test Results of Ø29 Ball Size Inner Tie Rod .....	50
4.2 New Small Diameter Axial Bearing Design.....	56
4.2.1 Oven Tempering Test Results .....	56
4.2.2 Ball Tempering Test Results .....	62
<b>5 Conclusion.....</b>	<b>72</b>
<b>6 References .....</b>	<b>74</b>
<b>7 Appendix A Measurement Results of the Groups.....</b>	<b>79</b>
<b>Curriculum Vitae .....</b>	<b>84</b>

# List of Figures

Figure 1.1: Steering system position in a passenger car [1].....	3
Figure 1.2: Rack and pinion mechanical steering system and its parts. [1] .....	4
Figure 1.3: Section cut of a hydraulic power-assistant rack and pinion steering system [1] .....	6
Figure 1.4: Electrohydraulic steering system [2].....	7
Figure 1.5: Outer tie rod, inner tie rod, and counter nut [1].....	8
Figure 1.6: Inner tie rod subcomponents.....	9
Figure 1.7: Outer tie rod subcomponents.....	10
Figure 1.8: Different outer tie rod design types [1] .....	11
Figure 1.9: Installation position of the tie rod in a McPherson front axle .....	14
Figure 2.1: Tribology: types of friction mechanisms [16]. .....	18
Figure 2.2: Bucket-type ball race with two slits .....	22
Figure 2.3: Variation of specific wear rate of APK, POM, UHMWPE, PA66, and PPS + 30%GFR using 150 grit emery paper.....	23
Figure 3.1: Part of the inner tie rod assembly, from left to right: ball stud, housing and ball race. ....	27
Figure 3.2: Inner Tie Rod assembly process.....	28
Figure 3.3: Schmatic view of assembly table.....	29
Figure 3.4: Tempering Oven.....	30
Figure 3.5: Carrier cabin .....	31
Figure 3.6: Ball tempering .....	32
Figure 3.7: ITR Housing .....	34

Figure 3.8: ITR Ball Stud.....	35
Figure 3.9: Functional diagram.....	35
Figure 3.10: Test sample selection demonstration.....	37
Figure 3.11: Articulation torque measurement .....	39
Figure 3.12: Articulation torque measurement device.....	40
Figure 3.13: Axial travel measurement device .....	41
Figure 3.14: Loading of ITR during measurement [9].....	42
Figure 3.15: Force-Displacement Curve [9] .....	43
Figure 3.16: Setting test .....	45
Figure 3.17: Setting Test Rig .....	46
Figure 3.18: Wear test figure [9].....	47
Figure 3.19: Wear Test Rig.....	48
Figure 4.1: Batch 0 change in $S_{ax}$ , $C_{min,ax}$ , and $M_k$ before and after the wear test .....	52
Figure 4.2: Batch 0 change in $S_{ax}$ , $C_{min,ax}$ , and $M_k$ before and after the setting test ...	54
Figure 4.3: Batch 1 change in $S_{ax}$ , $C_{min,ax}$ , and $M_k$ before and after the setting test ...	57
Figure 4.4: Batch 2 change in $S_{ax}$ , $C_{min,ax}$ , and $M_k$ before and after the wear test .....	59
Figure 4.5: Batch 2 change in $S_{ax}$ , $C_{min,ax}$ , and $M_k$ before and after the setting test...	61
Figure 4.6: Batch 3 change in $S_{ax}$ , $C_{min,ax}$ , and $M_k$ before and after the wear test .....	63
Figure 4.7: Batch 3 change in $S_{ax}$ , $C_{min,ax}$ , and $M_k$ before and after the setting test...	65
Figure 4.8: Batch 4 change in $S_{ax}$ , $C_{min,ax}$ , and $M_k$ before and after the wear test .....	68
Figure 4.9: Batch 4 change in $S_{ax}$ , $C_{min,ax}$ , and $M_k$ before and after the setting test...	70

# List of Tables

Table 2.1: Properties of POM at room temperature [17] .....	21
Table 3.1: Ø29 Inner tie rod production properties.....	34
Table 3.2: Inner tie rod production variants.....	38
Table 3.3: Setting test acceptance criteria.....	46
Table 3.4: Wear test block cycle.....	48
Table 3.5: Acceptance criteria before and after wear test.....	49
Table 4.1: Batch 0 functional measurements of Ø29 ball size before and after the wear test .....	51
Table 4.2: Batch 0 functional measurements of Ø29 ball size before and after the setting test .....	53
Table 4.3: Batch 1 functional measurements of Ø26 ball size before and after the setting test .....	56
Table 4.4: Batch 2 functional measurements of Ø26 ball size before and after the wear test .....	58
Table 4.5: Batch 2 functional measurements of Ø26 ball size before and after the setting test .....	60
Table 4.6: Batch 3 functional measurements of Ø26 ball size before and after the wear test .....	62
Table 4.7: Batch 3 functional measurements of Ø26 ball size before and after the setting test .....	64
Table 4.8: Batch 4 functional measurements of Ø26 ball size before and after the wear test .....	67
Table 4.9: Batch 4 functional measurements of Ø26 ball size before and after the setting test .....	69

# List of Abbreviations

APK	Aliphatic polyketone
$S_{ax}$	Axial travel, Spring travel
$C_{min, ax}$	Axial stiffness
EAA	Ethylene/acrylic acid copolymers
HDPE	High Density Polyethylene
ITR	Inner Tie Rod
LLDPE	Linear low-density polyethylene
$M_k$	Motion torque
OTR	Outer Tie Rod
POM	Polyoxymethylene
PTFE	Politetrafloroetilen
TR	Tie Rod
UHMWPE	Ultra High Molecular Weight Polyethylene

# Chapter 1

## Introduction

In the automotive industry, demands for lighter, more durable, and cheaper components are increasing by the leading automotive companies. To fulfill these demands, engineering calculations that have proven their competence at the design stage are required. They are actively used in the design of the systems that create the automobile.

The steering system is the system that transmits the circular motion from the steering wheel to the wheels linearly with the help of steering gear. The most crucial mechanical connection part of the steering system is the rods. The tie rod's most crucial function is transmitting the linear motion from the steering system to the knuckle.

The tie rod is an essential part of the steering system and a critical component from the safety point of view. It conducts the connection between the wheel and the steering system. A tie rod is simply an assembly of the inner tie rod and outer tie rod connected by a thread connection and a counter nut. By the thread connection, the tie rod length can be adjusted.

Tie rods can be damaged in many ways during operating, and these damages mostly cannot be recognized. One of these damages is the plastic bearing's wear or breakage inside the inner and outer tie rod assembly.

Starting in the last decade, customer load requirements for tie rods are significantly increasing. To obtain an accurate test result for these requirements, tie rods must pass the tests in terms of necessary loads and cycles, which are defined by auto manufacturers. Considering the customer requirements, the plastic bearing strength of

the tie rod assembly should also be considered. During this evaluation, plastic bearing strength should be checked by calculations.

During the design phase, the evaluations made indicate that the plastic bearing of the inner and outer tie rod is broken before completing the wear or setting test requirements. In this case, a bigger ball size is to be chosen to ensure the ball joint is safe from the requirement point of view. Bigger ball size has disadvantages such as heavier design and more expensive product cost.

In this study, a new bearing system (also known as ball joint) is developed to fulfill the defined requirements with a smaller ball size, leading to a lighter and cheaper design. Different press forces, tempering methods and tempering temperatures have been considered to reach the defined design targets during the study.

## 1.1 Steering System

The steering system serves to guide the vehicle under all driving conditions accurately. The driver's rotation movement to the steering wheel ensures that the front wheels are steered with other parts that make up the steering system. Figure 1.1 shows the position of the steering system in a passenger car. The steering system should be robust and precise and give the driver a sense of driving about various vehicle parameters. It is essential for the driver to continually feel the forces acting between the wheels and the road. This data is transmitted to the driver by the torque acting on the steering system. For this data to be transmitted effectively, there should be as little friction as possible at the steering system powertrain.

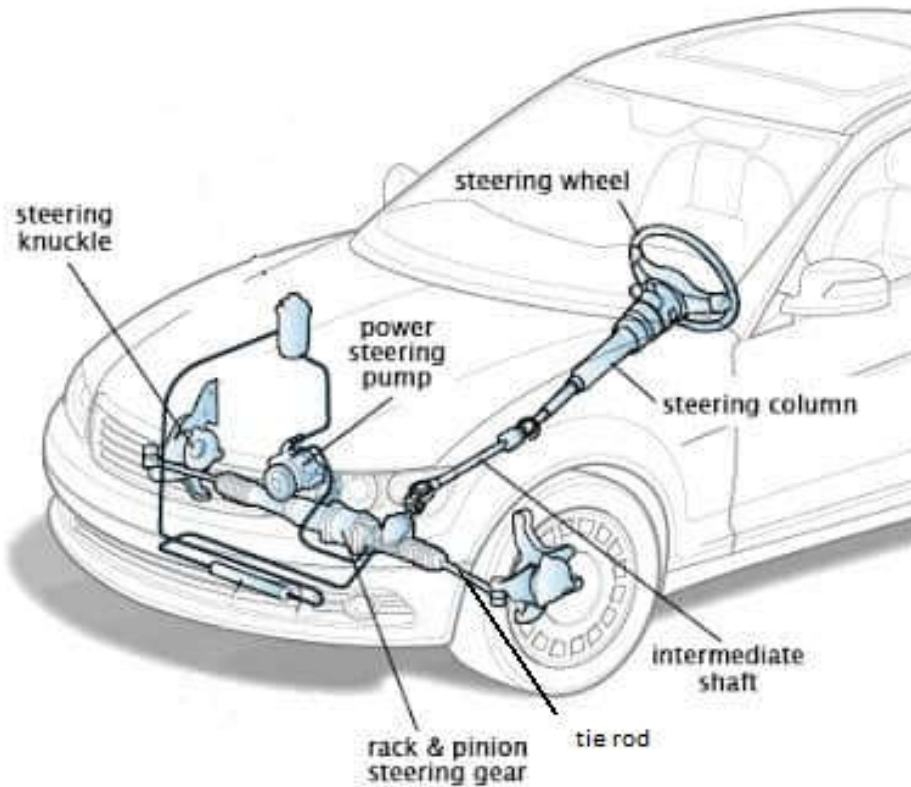


Figure 1.1: Steering system position in a passenger car [1].

A steering system consists of the steering wheel, steering column, intermediate shaft, power steering pump, rack & pinion steering gear, tie rod, and the steering knuckle. The tie rod is connected to the steering knuckle by ball joints. The intermediate shaft rotates with the steering wheel's rotational movement applied by the driver. As a result, power is transmitted to the steering gear. Rotational movement applied from the steering wheel by the driver is converted into linear motion by a gearbox. It transmits this linear motion over the tie rod to the knuckle and wheels.

The systems used to guide the vehicles have developed from past to present. More complex, easy-to-use systems have replaced simple systems. One of the most commonly used mechanical steering system designs is the rack and pinion steering system, and they are mostly used in light vehicles [2].



The steering system has two main categories, mechanical steering system and power reinforced steering system. In mechanical steering systems, the full rotation movement force should be applied by the driver. However, in power-reinforced steering systems, the rotational movement is supported by hydraulic or electronic power reinforcement, which requires less power to apply.

### 1.1.1 Mechanical steering systems

The steering movement applied by the driver to the steering wheel is transmitted to the wheels via the steering column, steering gear, and inner & outer tie rod. In this system, the driver's rotation movement to the steering wheel is transmitted to the steering gear. This circular motion is turned into linear motion with the help of rack and pinion. This linear movement is transferred to the tire by transferring the route. Figure 1.2 shows the rack gear steering system and its parts.

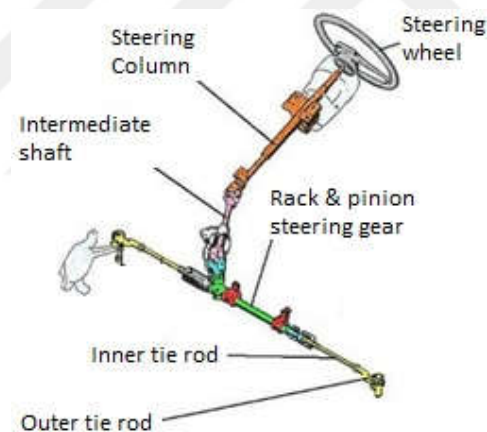


Figure 1.2: Rack and pinion mechanical steering system and its parts. [1]

The mechanical steering system has some disadvantages. In this system, the driver's force to turn the steering wheel is high, and the system's response during motion transmission is slower. Driving sensation is reduced at high speeds [3].

## 1.1.2 Power reinforced steering systems

As a result of technology development, cars' performance has shown a rapid change and development. New powerful and fast vehicles have become more difficult to control, and consequently, power-assisted steering systems have been designed to assist the driver. Hydraulic powered reinforced steering systems have been designed as the first of these. Today, besides these hydraulic power-assisted steering systems, electrical assisted systems are also used.

Due to the broad base and low air pressure tires used in modern cars, tire friction increases, and more steering force is required to steer the vehicle. In hydraulic power-assisted steering systems, hydraulic pressure application is used as an aid for the driver to guide the vehicle. This pressure provides the necessary power to move the wheels. The power required by the driver to the steering wheel is significantly reduced. The pressure is increased at higher force requirements. The change in this pressure is provided by a control valve connected to the main steering shaft. Figure 1.3 shows a schematic picture of the pinion, rack, and hydraulic cylinder.

Power steering systems have several disadvantages. The number of parts increases, and the cost increases with new additional systems in the power steering system. The fuel economy is badly affected by the hydraulic pump. Also, it is difficult to turn the steering wheel when the engine is at a standstill.

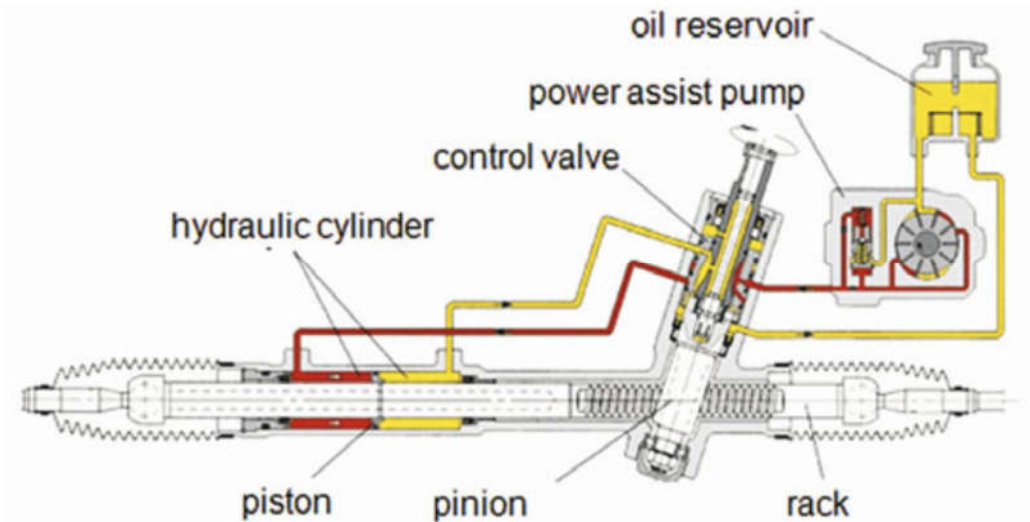


Figure 1.3: Section cut of a hydraulic power-assistant rack and pinion steering system [1]

While the hydraulic power-assisted steering system has many advantages over the mechanical steering system, they also have some disadvantages in fuel consumption. In these systems, the engine provides the operation of the pump, which increases fuel consumption. To prevent high consumption, the electrohydraulic power reinforced steering system has been developed. In this system, the hydraulic pump's power is provided by the electric motor, thus saving fuel. The battery provides the energy of the electric motor.

Compared with the hydraulic power-assisted steering system, up to 4% improvement in fuel economy may occur with in this system [3]. Figure 1.4 shows an electrohydraulic steering system.



Figure 1.4: Electrohydraulic steering system [2]

In electric power-reinforced steering systems, driver rotates the steering wheel to steer the vehicle, this movement force is increased by an electric motor. The driver applies less torque than needed in the hydraulic steering system. Electric powered-reinforced steering systems provide more fuel savings than electro-hydraulic powered reinforced steering systems. [3]

Electric power-reinforced steering systems are powered entirely by electricity to provide battery-powered steering in a challenging manoeuvre even if the engine is stopped. Advances in the field of sensor and control have created a favourable environment for electric power-reinforced steering systems. Sensors measure the angle of rotation the driver applies to the steering wheel and its direction. In this way, the magnitude of the support power to be applied from the electric motor is determined. Electric power-reinforced steering systems are frequently encountered in new-generation vehicles.

## 1.2 Steering Tie Rods

The steering tie rods connect the steering rack to the steering knuckle so that the steering commands given by the driver can be transmitted to the wheels [1]. It provides

transmission between the steering gearbox and the knuckle in steering systems. In this way, the steering from the driver can be transmitted to the wheels.

In driving conditions, the wheels also move vertically parallel to the steering axis; this system is under the influence of a force in the third dimension. Therefore, the use of ball joints in rods is required. The inner tie rod, located at the steering gear side, has an axial ball joint, while the outer tie rod on the knuckle side has a radial ball joint as shown in Figure 1.5. With the help of the ball joints, the left and right horizontal movement and the up and down vertical movement of the wheel can be provided.

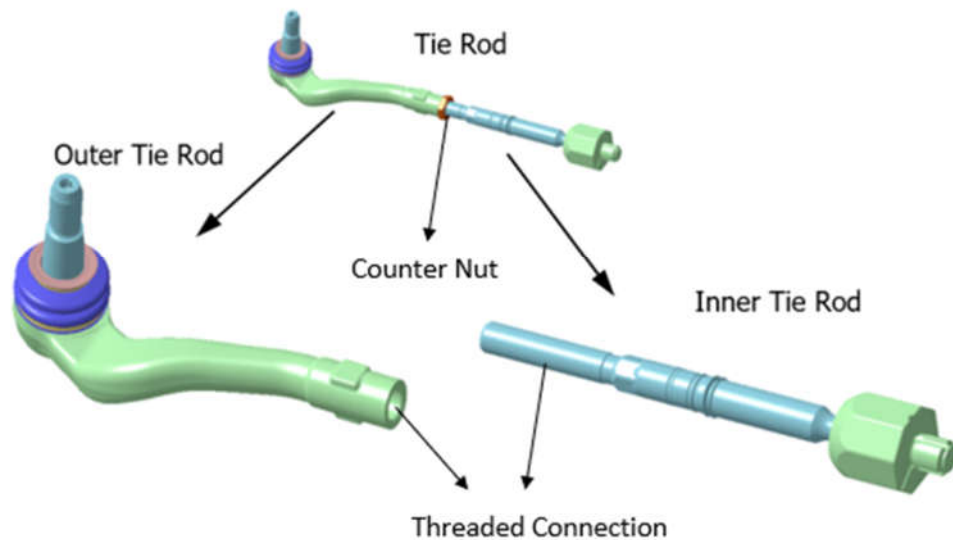


Figure 1.5: Outer tie rod, inner tie rod, and counter nut [1]

It is essential to install the tie rod that the length can be adjusted around  $\pm 5$  mm to  $\pm 15$  mm for a better angle adjustment. That is the reason why the tie rod consists of two thread connection parts. Tie rod assembly is also used as a fuse in the steering system. In such a case, the tie rod is expected to buckle before expensive parts of the steering system are damaged. The tie rod is expected to be deformed first in the failure chain since it is easier to replace than steering gear. When the tie rod is buckled after a high applied force, the driver can easily understand that the tie rod is buckled, therefore affecting the driving stability. The force to buckle the tie rod should be higher than the

force exposed to working conditions.

A tie rod is an assembly of the inner tie rod, outer tie rod, and counter nut. These three parts are mounted together with a thread connection. The inner tie rod provides the connection with the steering gearbox side, while the outer tie rod provides the connection with the knuckle. The outer tie rod is usually made of forged or cold-forged radial housing and includes a bearing part for the ball joint. Thread is opened on the end of the outer tie rod, as shown in Figure 1.5, to be attached to the inner tie rod and connected to the steering system. Ideally, it is desired to design the outer tie rod straight, but in some cases, curved designs can be used due to the position of other parts in the vehicle, such as the control arm. [4]

Inner tie rod includes axial housing, axial ball stud and plastic ball race. Figure 1.6 shows the assembly components of the inner tie rod. The inner tie rod is manufactured by the cold forging method. During the assembly of these single components by pressing operation, axial housing is subjected to plastic deformation under high load. The axial ball stud cannot easily get out of the axial housing. The ball stud can stay up to 40 kN pull-out force without separation from the axial housing [1].

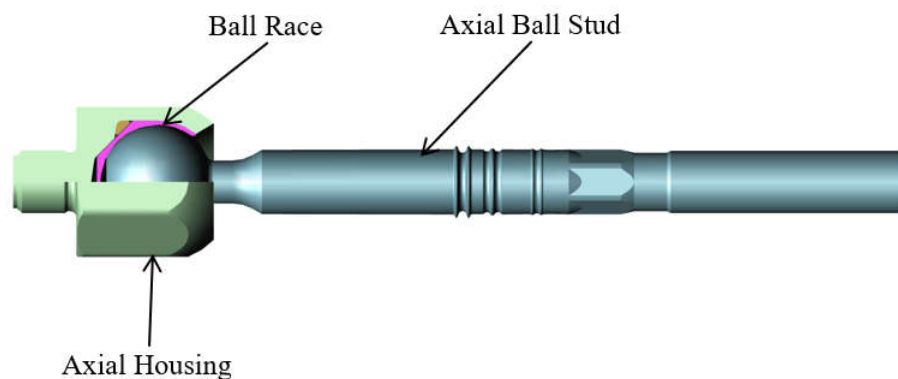


Figure 1.6: Inner tie rod subcomponents

The outer tie rod includes a spherical ball stud positioned perpendicular to the rod axis. The outer tie rod housing is usually manufactured by hot or cold forging. It has a bearing for the ball joint at knuckle connected side, and the connection is provided

with the thread in part to be connected to the inner tie rod. The ball joint connection is protected from dust and moisture through a sealing boot in a complete sealing system. There is grease between the bearing and the rubber. Figure 1.7 shows the outer tie rod subcomponents.

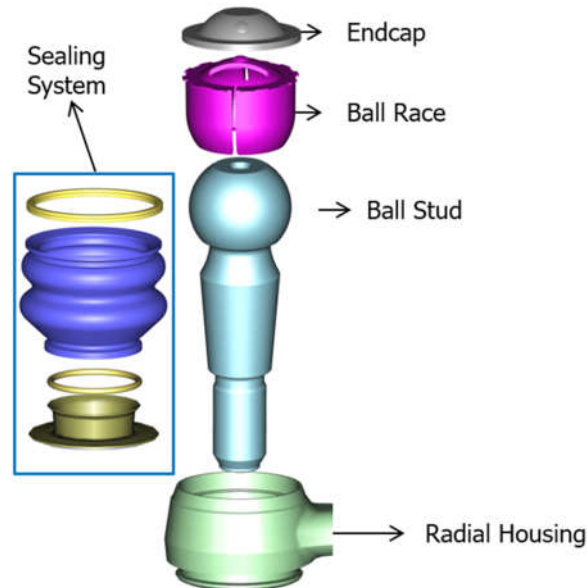


Figure 1.7: Outer tie rod subcomponents

In the most straightforward outer tie rod design, the outer tie rod's ball center coincides with the inner tie rod's ball center. This design is not always possible. Due to many other components around the tie rod, there are constraints on the tie rod's shape. Due to these package constraints, there are variations in the geometry of the tie rods. The sphere's location can be changed in one or more directions to comply with package constraints. Although the tie rod head is ideally flat, curved designs are also possible in some cases. Some types of curved designs are shown in Figure 1.8.



Figure 1.8: Different outer tie rod design types [1]

Since the tie rod's task is to transmit the steering movement to the wheels in the steering system, it requires a meticulous design and manufacturing process. Any malfunction in the tie rod can cause acoustic and stability problems while driving the vehicle. The force from the road is applied on the tie rods by the vehicle's movement, and the tie rod is expected to withstand this force and not to be damaged under specific critical loads [5]. These loads are the setting loads resulting from a suddenly increased loading that might damage the plastic ball race in the joints and the result of continuous driving conditions varying between usual and extreme driving conditions that might cause wear effect on plastic ball race.

In bad road conditions, especially over bumpy and ditchy roads, at specific forces applied by the suspension system, the tie rod can be damaged by fatigue forces or completely buckled [6]. Therefore, the tie rod is designed as a fuse element in this system to protect other expensive parts such as steering gear and knuckle.

The suspension and steering systems of the vehicle should be checked regularly. A worn inner or outer tie rod joint can cause unstable orientation and excessive tire wear. Some of the causes of tie rod damage are insufficient design, incorrect installation, overloading, unexpected stress-increasing factors, material defects in critical areas, inappropriate material or production method, and inappropriate heat treatments [7].



Tie rods are subjected to forces during vehicle steering. Under repeated loads, wear might occur in the plastic ball race, and as a result of high wear, the part is broken and damaged. Corrosion can cause damage when it occurs inside the ball joint. Simultaneously, the manufacturing method's inadequacy is one of the factors causing damage by neglecting many factors. Exposure of the rod to excessive force and sudden high impacts can cause damage.

The road comes with many repetitive loads. On a smooth road, the rod is subjected to lower amplitude forces, whereas, on rough roads, turns, pits, and roads characterized by humps, it is exposed to higher forces. It is necessary to consider such situations in the design and production process. In terms of safety, good performance, and long life, design and manufacturing stages should be prepared by taking many roads and driving scenarios into account.

Material density, strength, and costs are essential factors for choosing materials for tie rods. Press and pull forces are fundamental forces affecting the rod. At high compression forces, the rod may twist and cause damage. Therefore, yield strength is one of the critical factors for rod materials. Another critical factor is the weight, as the fuel consumption is proportional to it. Some of the outer tie rods are manufactured from heat-treated T6 aluminum material for weight reduction; however, using aluminum leads to higher costs. For these reasons, suitable materials for tie rods are generally high strength, low cost, and low-density materials such as steel parts out of cold or hot forging operation [8].

### 1.2.1 Inner Tie Rod (ITR)

The inner tie rod is a dynamically loaded component used as a connection element in the steering of a vehicle. It transfers the steering movements carried out by the driver to the wheel carrier via the tie rod.

Inner tie rod consists of three individual components: a ball stud, spherical ball race, and axial housing, as shown in Figure 1.6. Components are assembled on a fully automated rotary table; the final assembly station is the hydraulic or servo-electronic pressing operation. Axial housing and ball race are manufactured by external suppliers and used in assembly directly as they are purchased. Ball studs are manufactured by

external suppliers as raw ball studs. Before the assembly of the inner tie rod, ball stud neck and ball of the ball stud is machined fully automatically, as this area has very tight tolerances.

Ball stud is made from 30MnVS6 material by cold forming. After machining the ball and neck, the ball is smoothed by rolling, significantly reducing the spherical surface's surface roughness. This surface provides sufficient smoothness to wear resistance.

Spherical ball race has the most complex geometry because it is the most stressed part in the joint and serves as a bearing element between ball and housing. Ball race is manufactured by injection molding of the Thermoplastic POM Delrin® 100 material.

Housing is a cold-forged part made of the material C15E. The housing's outer contour corresponds to an octagon, which is for mounting on the steering gear rack. A sealing bellow covers the entire joint up to the steering rack to protect the joint from moisture and foreign objects. This protects the ball stud and housing from corrosion by preventing abrasive wear inside the joint. As mentioned initially, the tie rod serves primarily to execute the driver's steering movements from the steering gear to the knuckle. In this case, the inner tie rod is supposed to absorb axial forces, resulting from the cornering forces, which may occur when cornering fast or on uneven road surfaces or due to parking maneuvers.

An adjustment thread can adjust the tie rod; thus, creating an optimal driving condition is possible. This contributes to an improved running of the vehicle and reduced tire wear. In Figure 1.9, the mounting position of the tie rod in a McPherson Front axle is shown. The position or shape can vary depending on the space available in the front axle of the car.

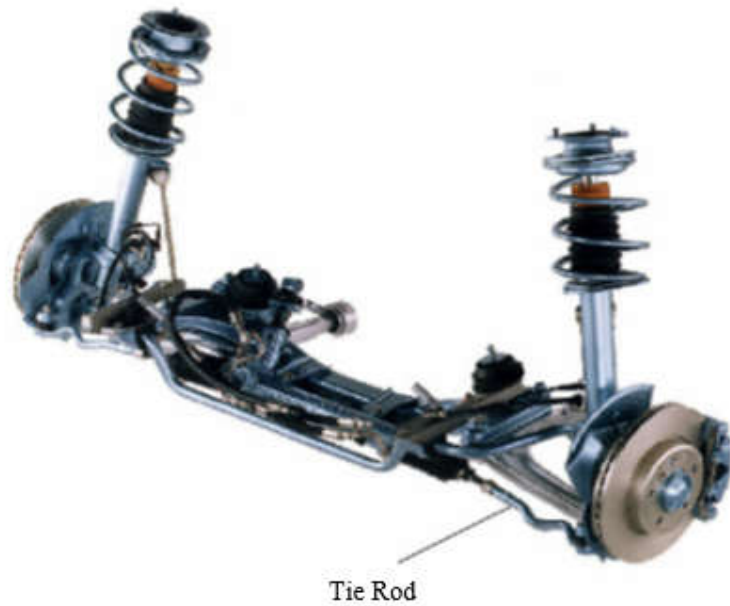


Figure 1.9: Installation position of the tie rod in a McPherson front axle

The following three requirements are the main specifications accepted by automotive manufacturers worldwide.

- (i) Articulation (tilting) torque: ( $M_k$ ) The moment of articulation is a characteristic value for sliding friction between ball and ball race after the joint's first breakaway movement. Tempering has a significant effect on the reduction of the moment of articulation. Torques are checked at articulation torque ( $M_k$ ) and expected to be in the range of 0.5 – 3.5 Nm. [9]
- (ii) Axial travel or Spring travel ( $S_{ax}$ ), which occurs between the joint housing and the ball race, in general, test force of  $\pm 3\text{kN}$  is determined. The maximum allowable travel is generally defined as 0.05 mm [9].
- (iii) Axial stiffness ( $C_{\min, ax}$ ): The stiffness of a joint is the minimum amount tangent slope in the flattest section of the curve defined and expected to be higher than 100 kN/mm [9].

### 1.3 Literature Review on Tie Rods

Özsoy and Pehlivan [10] carried out a structural analysis of a van type vehicle's body rod, spherical joint, and plastic bearing with finite element method. They included all assembly parts in the analysis and analyzed contact interactions between the parts. The analysis was carried out in different parameters according to the different mounting orientations of the rod head. With this modeling approach, each part's stress changes, and deformation characteristics were investigated for different loading conditions. As a result of the research, the maximum stress in the ball stud, the housing, and the ball race was 211, 160.8, and 9.1 MPa, respectively. Although the highest tensile value was on the ball stud, it was stated that the damage occurs on the housing, because ball stud was designed of AISI 5140 material with high yield strength and high tensile / life values.

Shende and Padole [11] examined the steering mechanisms of heavy commercial vehicles. They stated that sudden loads caused the most significant effect causing damage to the rod occur during steering the wheels. By making improvements in the rod's design in the series, they calculated the fatigue performance and durability life with the finite element method. As a result of their studies, they have determined that the bushes they add to the rod geometry reduce stresses.

Flores et al., in their study [12] investigated the effects of the joint gap on mechanical systems. They modelled the joints to include the actual characteristic gap, friction, and lubrication. To analyze the joint gap's effect, they analyzed the joints by frictionless dry contact, dry friction contact, and lubricated by three methods. As a result of numerical calculations, in the mechanisms where the spaces are modelled as dry friction, the forces are formed irregularly; They have seen that vibration and wear occur, causing durability problems. They stated that if the gaps are modelled as lubricated, the forces formed are more regular.

Zhao et al. [13] presented a method to predict the effect of the amount of gap in the rolling joints on wear. The elastic elements are modelled based on the absolute node coordinate formulation method, and the contact forces of the hinge components are calculated by the continuous contact method. The study in which the crank connecting rod mechanism, which has a rotating joint as an exemplary mechanism, was used, they

investigated the effects of the joint space on the impact of wear and impact in rigid and flexible modelling of the mechanisms. As a result of numerical calculations, it is found that the forces are formed irregularly in mechanisms modeled by dry friction of the gaps; They saw that vibration and abrasion occurred and this caused durability problems. They stated that when the cavities are modeled as lubricated, the resulting forces are more regular.

Mohamed et al. [14] aimed to determine the automotive pre-order system's workload under real conditions. The workloads were obtained by data collection operations on the test track. The information obtained from sensors such as accelerometer, wheel force sensor, and strain-gage were recorded with data collection systems. Factors such as load, vibration, stress, and noise affecting the McPherson suspension system were recorded under operating conditions. They arranged the data to be used in the fatigue/strength test system and damage analysis.

As summarized in literature view of tie rods, the studies have been done mostly related to finite element analysis. Studies have been done in respect to complete tie rod assembly including inner and outer tie rods. In this thesis, the ball joint of the inner tie rod has been considered and study have been done for improvement of the plastic bearing for smaller ball diameter. Literature review regarding bearing is presented in Section 2.3.

# Chapter 2

## Bearing System

A bearing system can be defined as any two components that contact and move with respect to each other and that have a common contact area as a point or a line. Friction and wear would occur in all bearing systems. The magnitude of this wear and friction depends on the related motion of the components. The study which considers friction and wear is named tribology. Regarding ball joints, it is necessary to decrease wear and friction to limit energy losses, extend service life and improve the connection function.

At the first bearing designs, there was no plastic ball race. As a result, steel balls used to damage the inner contour of housing. Together with the first created ball joints, the need of bearing system as lubrication raised. Production of the first maintenance-free ball joint is developed at the beginning of 1940. Usage of plastic ball race replaced the direct contact of steel surfaces. Even though the plastic ball race has a weaker load carrying capacity, no additional lubrication is necessary. These days all ball joint connections are manufactured as maintenance-free. With the help of the sealing system, dirt and water ingress is also avoided [1].

### 2.1 Wear Mechanism in Bearing Systems

Tribology encompasses interacting surfaces' fundamental science and technology under relative motion. Thus, it deals with the penetration of all types of friction, wear, lubrication, and the technical application of tribological knowledge. The tribulation system consists of basic and counter bodies as well as intermediate and ambient medium (usually lubricant and air). The sum of the external load effects, such as process forces, temperature, or sliding speed, forms the tribological stress cycle. If the

tribological conditions within a forming process are precisely known, then friction and wear can be minimized by a suitable selection of the individual tribological system components [15]. Figure 2.1 shows the different friction mechanisms.

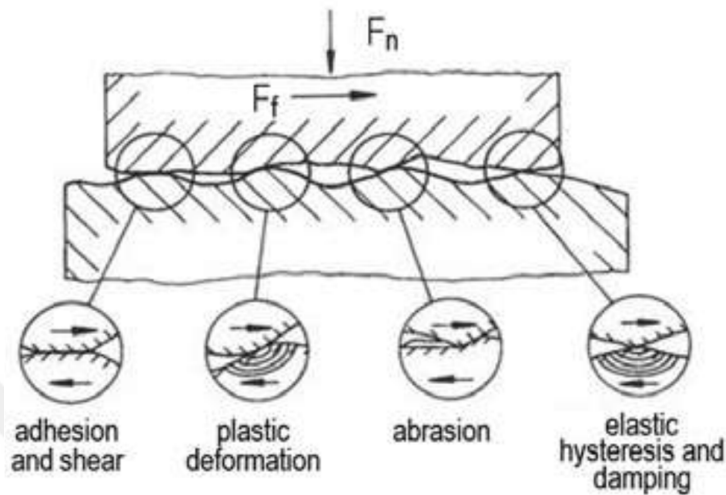


Figure 2.1: Tribology: types of friction mechanisms [16].

## 2.2 The wear system

If two contacting material areas perform relative movements, friction occurs in their common boundary surface - due to mutual interactions. The dynamic friction describes the force that counteracts the contacting body's relative motion and leads to the loss of mechanical energy. This energy loss is often undesirable and is reflected by the generation of heat energy that leads to the heating of the contacting material areas. If the two material areas are solid bodies, friction processes between them are generally associated with wear. Wear is defined as a progressive material loss of the surface of a solid body caused by mechanical causes, i.e., contact and relative movement of a solid, liquid, or gaseous counter body. The wear is expressed in the occurrence of loose small particles (wear particles) and material and shape changes of the tribological surface [15].

During the general wear process, the physical and chemical processes can essentially be traced back to the following four wear mechanisms: adhesion, abrasion, fatigue,

and tribochemical wear.

In consideration of joint wear, the most relevant influence must be assigned to abrasion wear. Adhesion, fatigue, and tribochemical wear are negligible in contrast [15].

Adhesion wear can be described as a result of local contacts of the surfaces of two partners, leading to local welding and relative movement, with particle separation [17].

However, this type of wear has no significant influence on the wear behaviour of the axial joints.

Abrasive wear occurs when peaks of a significantly thinner counter body or hard particles grind the base body as a middle part and wear it in the form of microchips. Accordingly, a distinction is made between anti-grain and particle grading. The countercurrent can be caused by a rough counter body of appropriate hardness but by hard two-phase particles in it. Particle grading is pronounced when contact between metal and loose mineral particles is smooth in the surrounding medium. The hard particles may be contaminants incorporated into the sliding gap or wear particles formed by adhesion wear and not transported out of the sliding gap.

Therefore, abrasion wear requires a sufficiently large difference in hardness between the friction partners, as is generally the case between metals and minerals. Abrasive wear markings are mainly reflected in scratches and score marks [18].

Fatigue wear, also referred to as surface stiffening, is the consequence of cyclic surface stress, as is the result, for example, of repeated Herzscher compression under the influence of microplastic processes. If the fatigue limit is exceeded locally in such stressed surface areas, fatigue cracks develop, leading to the fracture of individual material parts during further growth. Therefore, pits (pitting) and cracks are marked for fatigue wear.

Pitting usually follows the total failure of the affected component rapidly. Tribological alternating loads are available, e.g., for roller, rolling, impact, and impact wear. Gears and antifriction bearings are, for example, also at risk due to fatigue wear. Fatigue wear can also occur on plain bearings, even in hydrodynamic lubrication conditions, if correspondingly critical vibrations from the bearing stud to the bearing shell via the



lubrication film. For example, sandblasting causes fatigue wear in vertical impact, but mainly abrasive wear in case of oblique impact [18].

Tribochemical wear involves chemical reactions between one or both friction partners and components of an intermediate material that would only occur due to friction activation of the surfaces and would not occur without tribological stress. The hardness of the tribochemically formed reaction products compared to the friction partners' hardness is of great importance for further wear development. Suppose the hardness difference is low or the reaction products are even softer. In that case, they can form a non-metallic separation layer between the friction partners and prevent generally severe adhesion wear. In this case, tribochemical reactions are favorable to wear behaviour. However, if relatively hard shifts occur, they are generally divided into wear particles, resulting in increased abrasion wear.

Tribochemically formed reaction layers are also undesirable if they add or even prevent the gap between sliding partners and make function-related relative movements between them more difficult. A known example of tribochemical wear is friction corrosion [18].

### 2.2.1 Properties of polyoxymethylene (POM)

POM material is used most commonly in inner tie rod ball joints [2]. Polyacethylene is also referred to as polyoxymethylene, which is named as the code POM. Since 1958, POM has mainly been manufactured by Copolymerization (the combination of different basic formulas) of trioxane and another monomer (X-ray substance or basic molten). There are both homo- and copolymerisates, which differ mainly because there are better thermal stability and higher chemical resistance in the Copolymerisats. The bearing shells used in the tie rods consist of the polyacetal Delrin® 100 from the manufacturer Du Pont and are manufactured using injection molding technology. Other trade names are Hostaform (Hoechst) and Ultraform® (BASF).

As has already been mentioned, the plastic material POM belongs to the thermoplastics group. It has a partial crystal structure with a high degree of crystallization (up to 80% of the crystal content of the homopolymerisate) [19].

POM has many outstanding characteristics that prove to be the best bearing material for the axial joints. However, this study only deals with setting and wearing tests on ball joint performance and the effect on ball race made of POM. These are listed in Table 2.1 below. Further characteristics can be found in the literature mentioned above.

Table 2.1: Properties of POM at room temperature [17]

<b>Property</b>	<b>Value</b>
Density	1.41 g/cm <sup>3</sup>
Melting temperature	175 - 185 ° C
Tension at the yield limit	67 - 72 N/mm <sup>2</sup>
Elongation at the yield limit	25 - 70 %
Modulus of elasticity	3200 N/mm <sup>2</sup>
Usage temperature (short-term)	110 - 140 ° C
Usage temperature (long-term)	90 - 110 ° C
Water absorption	0.80 %

POM is characterized, among other things, by high strength, stiffness, and toughness (impact resistant down to -40°C), low water absorption capacity, good sliding and wear behaviour, and good processability. Both the strength and stiffness of POM workpieces are more significant in a temperature range of 50 to 120 ° C compared with many other thermoplastics.

Therefore, POM is an excellent bearing material for axial joints over an extensive temperature range. At room temperature, POM has a significant flow transition at approximately 8 to 10% elongation. Below the flow transition, POM has excellent resilient properties (resilience) even with repeated loading and is therefore particularly suitable for producing resilient components and use in axial joints. [4]

POM is not hygroscopic and absorbs tiny water. This changes the physical properties of the molded parts only slightly. Its density is relatively high at 1.41 g/cm<sup>3</sup>, so that

POM workpieces are usually heavier than competing products made from other plastics. When developing new workpieces with POM, it must be noted that there is a shrinkage of approximately 2% due to crystallization effects. POM is strongly resistant to mineral oils, fuels (including those containing methanol and ethanol), and most organic solvents and hardly swells in these media. This makes it possible to lubricate the axial joints with a special grease additionally and to reduce wear. POM workpieces are characterized by perfect dimensional accuracy, strength, and toughness even under very high loads.

Due to the properties described, POM is the preferred engineering plastic in many industrial sectors. POM workpieces have also asserted themselves against other technical plastics in the automotive industry, device construction, and the electrical industry. They have become an indispensable part of the product range of many companies. POM workpieces are generally manufactured by injection molding and extrusion [21]. In Figure 2.2 an example of POM usage for ball race component is shown.



Figure 2.2: Bucket-type ball race with two slits

## 2.3 Literature Review on Bearing Systems

Unal et al. [22] performed an experimental study of APK, POM, UHMWPE, PA66, and PPS + 30%GFR polymers at 10 N load and different sliding distance reveals. According to the result of the study, it has been seen that the wear rate of APK, POM,

UHMWPE, PA66, and PPS + 30%GFR decreases with the increase in sliding distance. For all polymers used in this investigation, the specific wear rate decreases with the increase in grit grade number. Optical studies of worn surfaces indicate cutting, plowing, cracking wear mechanism under experimental conditions. Result graph of the study is shown in Figure 2.3

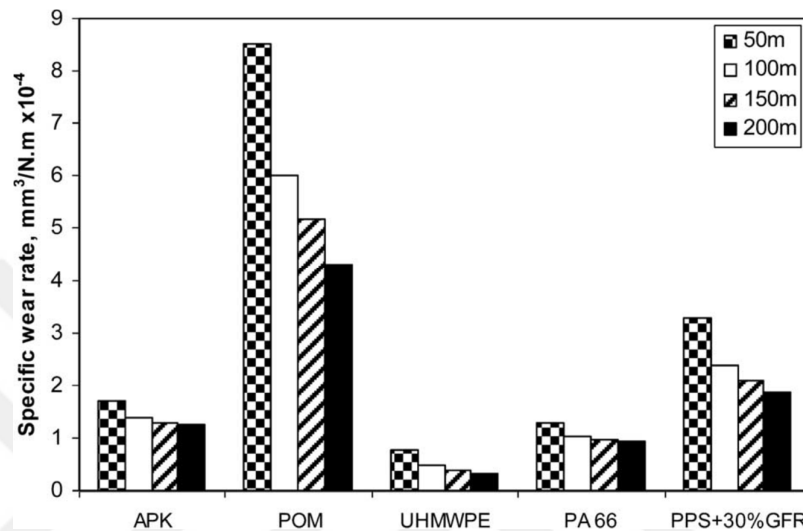


Figure 2.3: Variation of specific wear rate of APK, POM, UHMWPE, PA66, and PPS + 30%GFR using 150 grit emery paper.

The study shows that the highest wear rate is for POM polymer, and the lowest wear rate value is for UHMWPE polymer. However, market and technical requirements of ball race material show that POM is leading concerning the cost. [1]

Chen et al. [23] investigated the friction and wear behaviour of polyoxymethylene/linear low-density polyethylene/ethylene-acrylic-acid blends. Results showed that the friction and wear properties of POM were significantly improved after an amount of LLDPE and EAA was added. The friction coefficient and wear scar width of POM are much higher than those of POM/LLDPE/EAA blends under the same condition. The SEM analyses show that POM and POM/LLDPE/EAA blends exhibit different wear mechanisms. The transfer film of POM is formed on the surface of the steel counterpart. For POM/LLDPE/EAA blend, the lamellar debris is found on the steel ring surface sliding against POM/LLDPE/EAA blend, decreasing

the friction coefficient and wear scar width. The lubricating layer formed in the contact surface prevents the bulk from severe wear. Therefore, the POM/LLDPE/EAA blend's friction coefficient was reduced remarkably, and the anti-wear property got greatly improved. The study shows that the steel part's continuous movement on POM without additional materials would have a high wear impact on POM material. This is a similar case of wear test applied in Section 4.3 and can answer the reason of high impact on functional measurements

Unal and Mimaroglu [24] investigated the friction and wear behaviour of unfilled engineering thermoplastics. Based on the results of dry friction and wear tests, they found out that the wear rates of polyamide 6 and UHMWPE were in the order of  $10^{-6}$  while for POM, it is in the order of  $10^{-5}$  mm<sup>3</sup>/Nm at the range of load and speed studied in this work. Polyamide 6 friction coefficient values, UHMWPE, and POM slightly increase with load. The highest specific wear rate was observed in POM, and the lowest is for UHMWPE polymer. In general, the wear rate is not influenced by the change in load. For the specific range of load and speed explored in this study, the speed has a more substantial effect on the wear rate of polyamide 6, UHMWPE, and POM than the load. Worn surfaces for POM, UHMWPE, and polyamide 6 are wrinkled and grooved, respectively.

According to the study, since the wear effect on the POM material is increased by speed, the planned wear test block cycle collective shown in Table 3.4 would have more severe wear damage on higher test frequencies.

Kırlı [25] investigated POM material properties used in ball joints and studied on a model to create a finite element analysis model. He investigated the effect of different temperature levels on POM material on the level of stress and displacements with compression loads, after the finite element analysis and real part test results are compared, and a new finite element analysis method is created.

During the study, the test piece's compression tests were applied at -60°C, -40°C, -20°C, 0°C, 23°C, 50°C, 80°C, 100°C, 120°C temperature levels. Also, these results were compared with the results of the tensile test. In conclusion, it was observed that high temperatures change the behaviour of the POM material. In the scope of the study, higher wear effect was expected at 80 °C.

Gao et al. [26] investigated contact of polymer-stainless steel with wear and friction tests. As a result of their analysis, they found that during the friction process, on surfaces complex chemical reactions occur. These reactions affect the polymers' wear and friction properties. They stated that because of the polymer transfer caused by reactions, characteristic structure of the polymer was affected. Wear and friction properties of the polymer is affected because of the transfer film. They underlined that in the polymers they examined the nylon 6, at 98 N load and 0.42 m/s test conditions, the friction coefficient was smaller than the initial PTFE ( $\gg 0.05$ ) but after 70 minutes increased to the level of 0.56. They imputed the low friction coefficient before start of film formation, the stiffness of nylon's to be greater than PTFE, and by this to a smaller contact area sustained. It is also evident that the steel-polymer contact creates wear on the ball race material.



# Chapter 3

## Material and Method

Details of the material used, and the methods followed are as follows.

### 3.1 Material

In this study, a new small diameter axial bearing is designed to resist high wear loads. After assembly, the pressing force for joint assembly is defined, the tempering method and temperature are determined to maintain the appropriate stiffness value to meet the wear loads of the axial bearing. Besides, the functional values as articulation torque ( $M_k$ ), Axial travel ( $S_{ax}$ ), Stiffness  $C_{ax, min}$ ) of the assembled inner tie rods are measured by experimental studies, and their wear behaviour is examined.

The effects of the standard pressing force and different tempering methods on the part's stiffness value are investigated. The inner tie rod assemblies with high stiffness are subjected to the wear test and the wear test results are compared, and an optimized design is obtained.

In the scope of the study, setting behaviour under maximum loading is also tested by the setting test. In this test, inner tie rods are loaded at maximum loading for three load cycles, and then functional measurements described below in Section 3.2.1 are applied. Setting test is described in Section 3.2.2.

Production and testing of the inner tie rods are done in ZF Lemförder Aks Modülleri San. ve Tic. A.Ş. Laboratories, Izmir

The following materials are used in this thesis study.

**Housing:** C15 acc. to EN 10277-2 (Bright steel products standard), case-hardened steel, manufactured externally by cold forging. Commonly used in the automotive market. [2]

**Ball stud:** 30MnVS6 acc. to DIN EN 10267 (Ferritic-pearlitic steels for precipitation hardening from hot-working temperature), micro-alloy steel, manufactured externally by cold forging. No additional heating process is needed after forging which brings cost advantage [3]

**Ball race:** plastic component POM. Commonly used in the automotive market [1]

The geometry of the components of inner tie rod is shown in Figure 3.1. These chosen single part materials mentioned above for each are the most commonly used in the market for inner tie rod production.

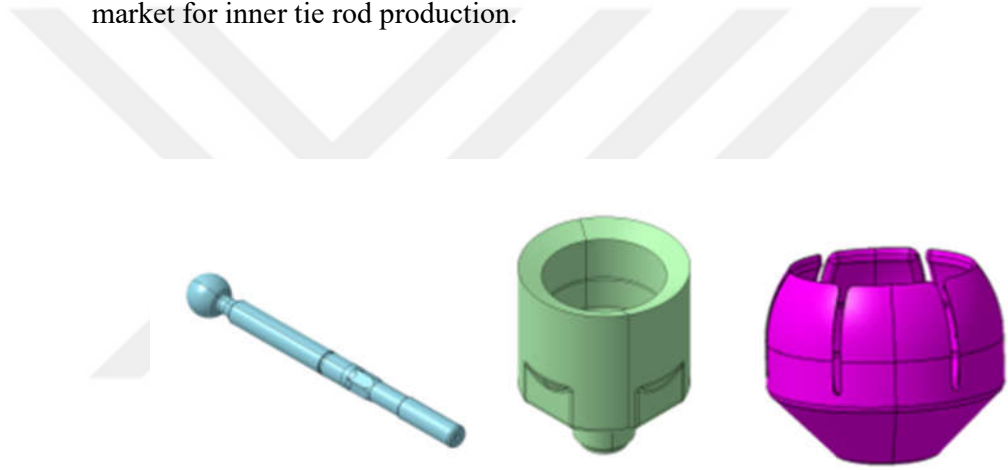


Figure 3.1: Part of the inner tie rod assembly, from left to right: ball stud, housing and ball race.

### 3.1.1 Assembly

Inner tie rod assembly components are ball stud, housing, and ball race. The components assembly process is shown below in Figure 3.2. The complete assembly process is done in ZF Lemförder Aks Modülleri San. ve Tic. A.Ş. Laboratories, Izmir



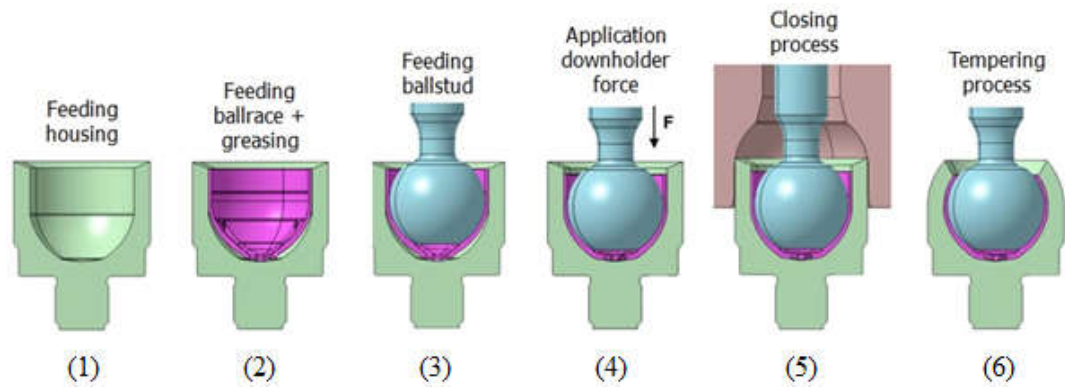


Figure 3.2: Inner Tie Rod assembly process

The assembly process can be explained in the following production steps,

1. Feeding housing on the assembly table.
2. Feeding ball race in housing and greasing the inner wall of ball race by a nozzle.
3. Feeding the ball stud into joint. (Ball tempering is done before feeding the ball stud in case of ball tempering method, as described in Section 3.2.1 Tempering)
4. Application of down holder force (around 2 to 4 kN) to keep all components stable during the closing process.
5. The closing process by applied force from the upper holder.
6. Tempering the joint in a tempering oven (Oven tempering is done in an oven separate from the assembly table. Process is described in Section 3.2.1 Tempering)

In this thesis assembly process number 3 ball tempering (only if ball tempering method is selected), number 5 closing force and number 6 oven tempering (only if oven tempering method is selected) are considered, and parameters are defined accordingly as described in Section 3.2 Method. Assembly on round table can provide around 30 assemblies per minute.

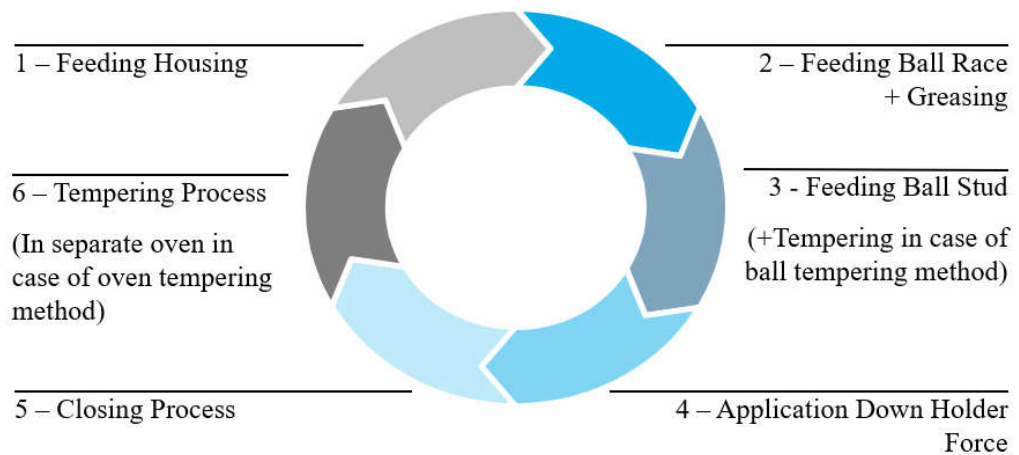


Figure 3.3: Schematic view of assembly table

### 3.2.1 Tempering

The tempering process enables the assembled housing, ball stud, and ball race to make surface contact with the temperature's effect, which is more suitable for the assembly parts. [27]

The articulation torque values of ball joints without the tempering process are high due to the high friction force. Therefore, to reach the desired torque values, the tempering is applied on complete inner tie rod or only on ball stud; thus, required articulation torque values are reached. [28].

Nevertheless, as a result of this heat treatment, while torque values decrease, axial and radial deflection increases. Therefore, tempering temperature and duration should be determined according to the inner tie's functional conditions.

There are two methods for the tempering process which are applied in this study

#### ➤ Oven Tempering

The complete inner tie rod is heated up to a defined temperature for a defined duration in the oven tempering option.

In Figure 3.4 tempering oven is shown. Oven is from company DBK Group, and maximum temperature rating is 150 °C with the electricity heating power capacity of 54 kW.



Figure 3.4: Tempering Oven

Inner tie rod assemblies are sorted in a carrier cabin as shown in Figure 3.5, which is open all around for maximum airflow and homogenous heat transfer. Assemblies are inserted in the oven manually by wheel moved cabin.



Figure 3.5: Carrier cabin

Oven tempering is applied after the complete assembly of the inner tie rods. During oven tempering, assembled inner tie rods lay on a tray, and the complete inner tie rod is heated up to a specific temperature. The main drawback with oven tempering is that, unnecessary areas of the inner tie rod are also heated up such as the ball stud shaft. This has no adverse effect on the ball stud but causes high energy consumption.

➤ Ball Tempering

Only the spherical ball is heated up to a defined temperature for a defined duration in the ball tempering option. The difference between oven tempering and ball tempering is that, in the ball tempering the ball is heated before feeding the ball stud during the assembly process. The machine used for this process is shown in Figure 3.6



Figure 3.6: Ball tempering

Ball tempering is applied directly at the assembly of the joint. In the production steps mentioned in the Section 3.1.1 Assembly, ball tempering is applied between the second and the third steps.

In this study, both tempering methods are investigated.

## 3.2 Method

In this study's scope, a new smaller ball diameter,  $\text{Ø}26$  mm axial bearing (ball joint) is developed. For the functional measurements, Spring travel ( $S_{ax}$ ), Stiffness ( $C_{min,ax}$ ), Articulation torque ( $M_k$ ) acceptance criteria are defined according to global ball joint standard [9].

The new  $\text{Ø}26$  mm axial bearing is compared with the current series product, a  $\text{Ø}29$  ball size axial bearing which has a larger ball diameter. The  $\text{Ø}29$  ball size product is

in series production and delivered to customers for many years as ZF Lemförder standard product. Ball diameter Ø29 inner tie rod is also measured for Spring travel ( $S_{ax}$ ), Stiffness ( $C_{min,ax}$ ), Articulation torque ( $M_k$ ) for comparison purpose.

In Section 3.2.1 Functional measurements, Section 3.2.2 Setting Test and Section 3.2.3 Wear Test is explained.

The study's target is to get the same functional performance from Ø26 ball size, which is already achieved by Ø29 ball size.

In this study 12 Ø29 ball size, and 180 Ø26 ball size samples in a total of 192 inner tie rod samples are manufactured, and functional performances are measured. According to the preliminary measurement results, 12 Ø29 ball size samples in 1 batch and 48 Ø26 ball size samples in 4 batches were used to focus on further wear and setting test. Each batch contains 12 samples, the first 6 samples are used for the setting test, and the second 6 are used for the wear test.

Inner tie rods are numbered according to the ball size, batch no, and sample no.

Numbering system is formulated as XX.Y.Z. In this case, XX symbolizes the ball size (Ø29 or Ø26), Y symbolizes the batch no (1,2,3 or 4), Z symbolizes the sample no (1 to 12 for each batch). For example, 26.2.8 is for sample no 8 from the 2<sup>nd</sup> batch of Ø26 ball diameter.

Inner tie rod production for Ø29 ball size has been completed with production conditions shown in Table 3.1. 12 inner tie rods are manufactured according to these conditions and this group of balls are named Batch 1. These conditions are directly the series production conditions that fulfill desired requirements by the customer. The “initial” tempering temperature is not given due to the commercial privacy policy of the Lemförder Company.

Table 3.1: Ø29 Inner tie rod production properties

Batch No	Press Force [kN]	Tempering Method	Tempering Temperature
0	Min press force	Oven	Initial

For the purpose of this study, a new small diameter axial bearing is designed with Ø26 ball size with a reduction of 3 mm in diameter.

The main dimensions of the housing and ball stud are shown in Figure 3.7 and Figure 3.8,

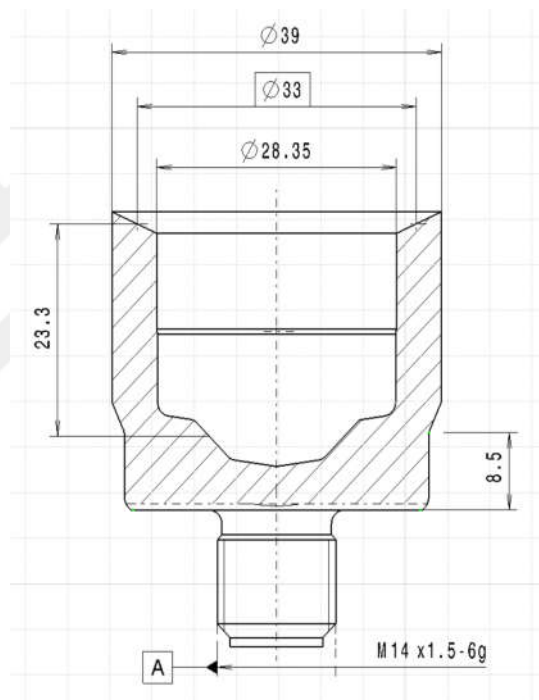


Figure 3.7: ITR Housing

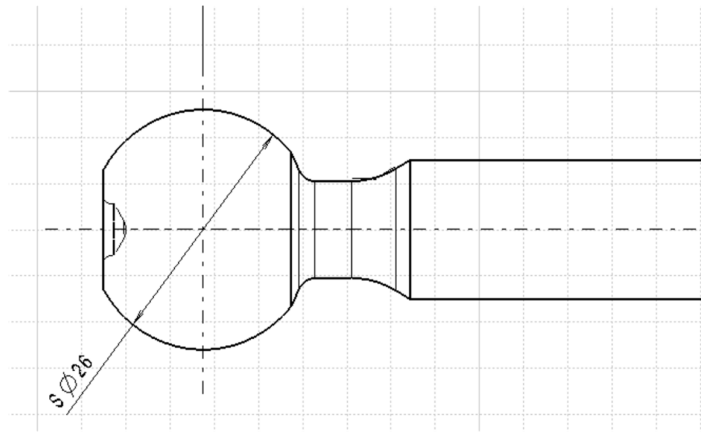


Figure 3.8: ITR Ball Stud

New smaller ball diameter  $\varnothing 26$  inner tie rods are produced according to three production parameters: press force, tempering method, and tempering temperature.

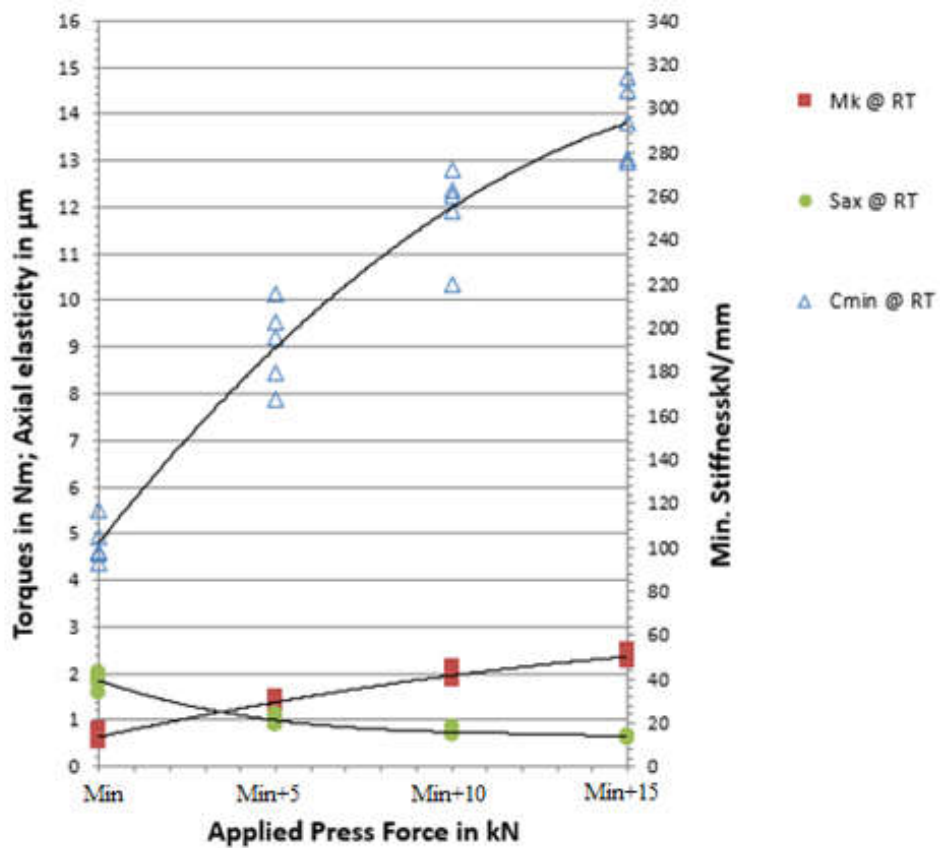


Figure 3.9: Functional diagram



During the test sample manufacturing, three different test groups are created. For each group creation, a new functional diagram is created, and an example diagram is given in Figure 3.9. Other diagrams could not be given due to privacy policy of the Lemförder Company. A functional diagram is created to involve all measurement results in one graphic for a summary. The “Min” applied force in Fig. 3.8 is not given due to the commercial privacy policy of the Lemförder Company.

On the left side of the graphic, the  $M_k$  and  $S_{ax}$  results; on the right side  $C_{ax,min}$  results, and the bottom side press force values are given. For every single functional diagram, only press force is increased 5 kN for each variant, and four variants have been created for each group by “increasing force” method. In the process of functional diagram creation, all assembled inner tie rods have been measured for  $M_k$ ,  $S_{ax}$ ,  $C_{ax,min}$  performance. After creating three different functional diagrams, one best variant from each group is chosen for testing.

In total, three different groups for the Ø26 ball joint are created. Before testing, all inner tie rods are measured for functional behaviour to identify  $M_k$ ,  $S_{ax}$ ,  $C_{ax,min}$  values. These measurements are repeated after wear and setting tests to ensure the inner tie rods fulfill the defined requirements. A summary table of the groups are shown in Figure 3.10. From each group, selected variants are highlighted in **bold**. Selected test variants are renamed as **Batch 1, 2, 3** and **4** for further testing.

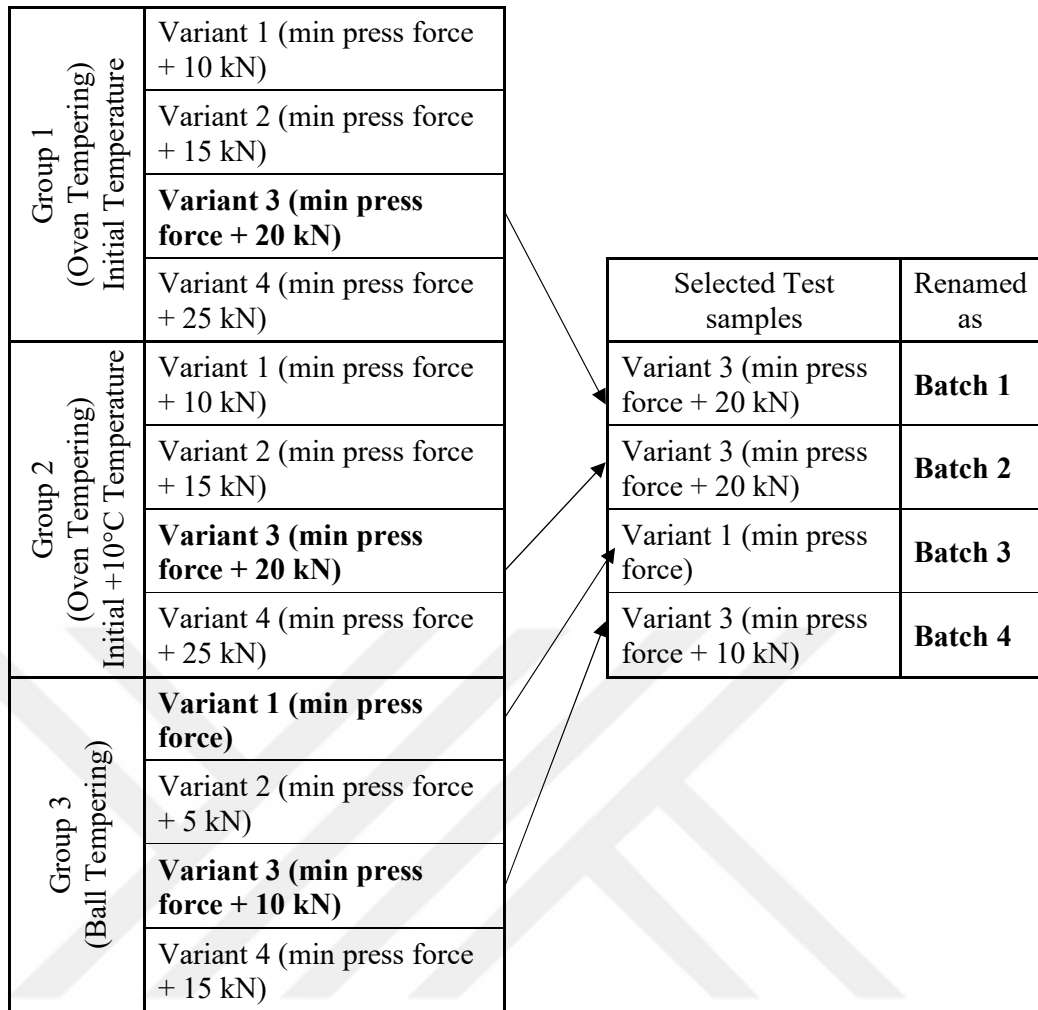


Figure 3.10: Test sample selection demonstration

For group 1 and 2, the tempering method is followed as oven tempering. Group 3 is tempered only by the ball. Detailed measurement results of all single assemblies are given in the Appendix A.

According to group 1 results, variants 1 and 2 failed at axial travel ( $S_{ax}$ ) measurement, variants 3 and 4 failed at  $M_k$  measurements. Since high  $S_{ax}$  before wear test would cause unacceptable results after wear test, variant 1 and 2 are not used for wear and setting testing, because wear on ball race will increase the axial travel. Variant 3 showed better articulation torque ( $M_k$ ) performance than variant 4 even with unacceptable results, it is planned to perform only setting test with this batch, and variant 3 has been chosen.

Group 2 assemblies are tempered in initial tempering temperature + 10°C since no additional improvement was possible to get acceptable results with Group 1 different pressing force variants. Higher tempering temperature can improve the articulation torque performance [18]. Group 2 measurement showed similar behaviour with Group 1 since variant 1 and 2 failed at axial travel ( $S_{ax}$ ) and variant 4 failed at articulation torque ( $M_k$ ). Variant 3 passed all the requirements and was chosen for further wear and setting testing.

Group 3 measurements showed unacceptable results only at variant 4 with articulation torque ( $M_k$ ). Variants 1, 2, and 3 were evaluated as sufficient. For testing variants 1 and 3 are chosen to test the upper and lower limit samples.

All chosen inner tie rods variants are summarized in Table 3.2, for each variant 12 inner tie rods are manufactured, and functional performances measured.

Table 3.2: Inner tie rod production variants

Batch No	Press Force	Tempering Method	Tempering Temperature
1	Min press force + 20 kN	Oven	Initial
2	Min press force + 20 kN	Oven	Initial + 10°C
3	Min press force	Ball	Initial
4	Min press force + 10 kN	Ball	Initial

### 3.2.1 Functional measurements

Functional properties of the inner tie rod assembly are Spring travel ( $S_{ax}$ ), Stiffness ( $C_{min,ax}$ ), Articulation torque ( $M_k$ ). These properties are specific for every single assembly, for this reason, all assemblies are measured before and after testing.

Throughout the thesis “functional values” means “motion torque, axial travel and axial stiffness values”.

### 3.2.1.1 Articulation Torque

The effect of different assembly and tempering parameters (press force, tempering method and tempering temperature) on the friction moment of the inner tie rod axial bearing was investigated by the articulation torque measurement. Before starting the articulation torque measurement, the ball stud of the inner tie rod is articulated 5 times in the direction of the working angle of the inner tie rod. This preparation is being done to establish the homogenous grease distribution at complete joint area. After the preparation, articulation torque measurements are performed at 10<sup>0</sup>/s articulation speed. During articulation torque measurement, the ball stud is articulated 5 times at  $\pm 22^\circ$  (80% of max articulation angle acc. to AK-LH-14). The torque is recorded as the measurement result [9]. In Figure 3.11 the articulation movement demonstration is shown, the arrow symbolizes the articulation movement. Tilting torque measurement device is shown in Figure 3.12.



Figure 3.11: Articulation torque measurement

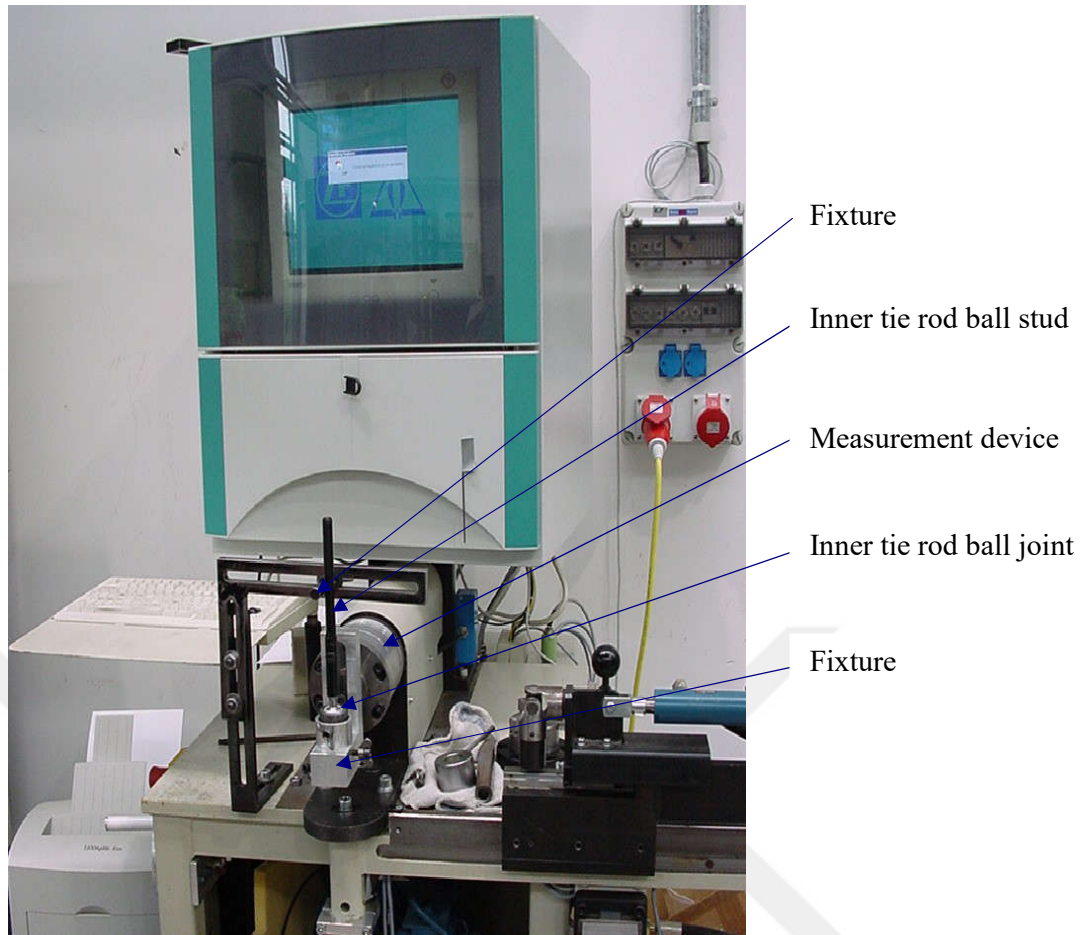


Figure 3.12: Articulation torque measurement device

### 3.2.1.2 Axial Travel

The axial spring travel  $S_{ax}$  is measured by a measurement device shown in Figure 3.13, with the test sample is attached to the machine's piston rod using connecting elements. The housing of the test sample is firmly fixed on the machine table. Measurement device is used to apply the axial force on the inner tie rod from ball stud to housing direction. By applying the defined axial force, the ball stud ball area inside the joint moves in the axial direction. The travel of the ball inside the joint is recorded.

According to the automotive standard AK-LH-14, the test force  $F_{ax} = \pm 3\text{kN}$  is applied sinusoidally with a frequency of 0.5 Hz. First, 3 preload cycles are carried out, which are then followed by the test cycle without interruption. Measurement is completed after the creation of hysteresis shown in Figure 3.14 as an example.

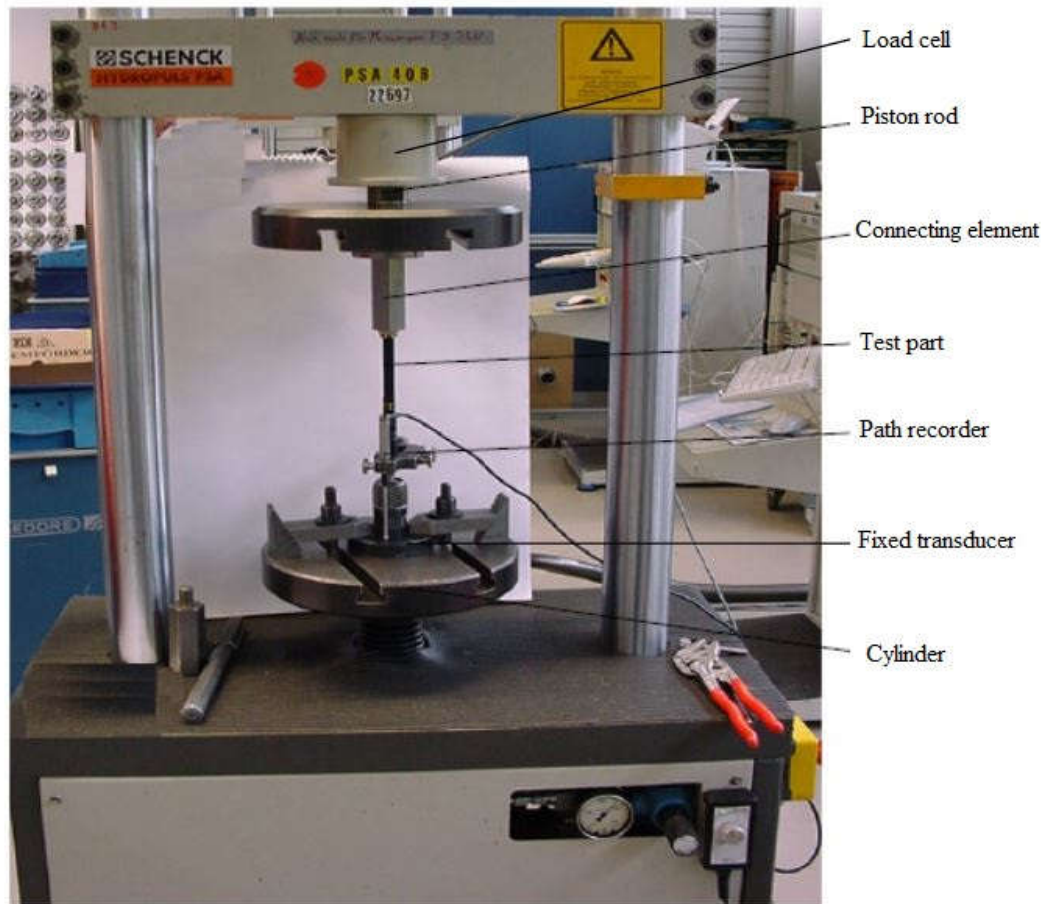


Figure 3.13: Axial travel measurement device

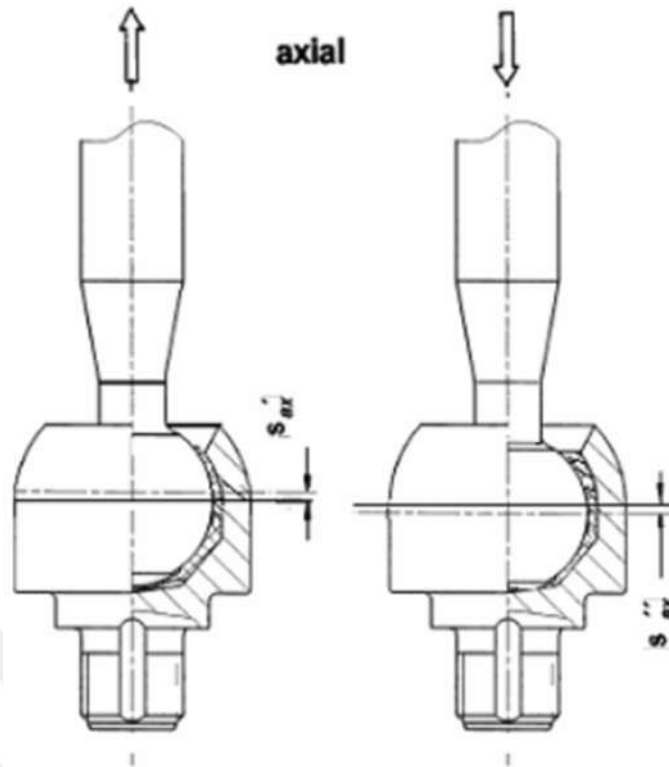
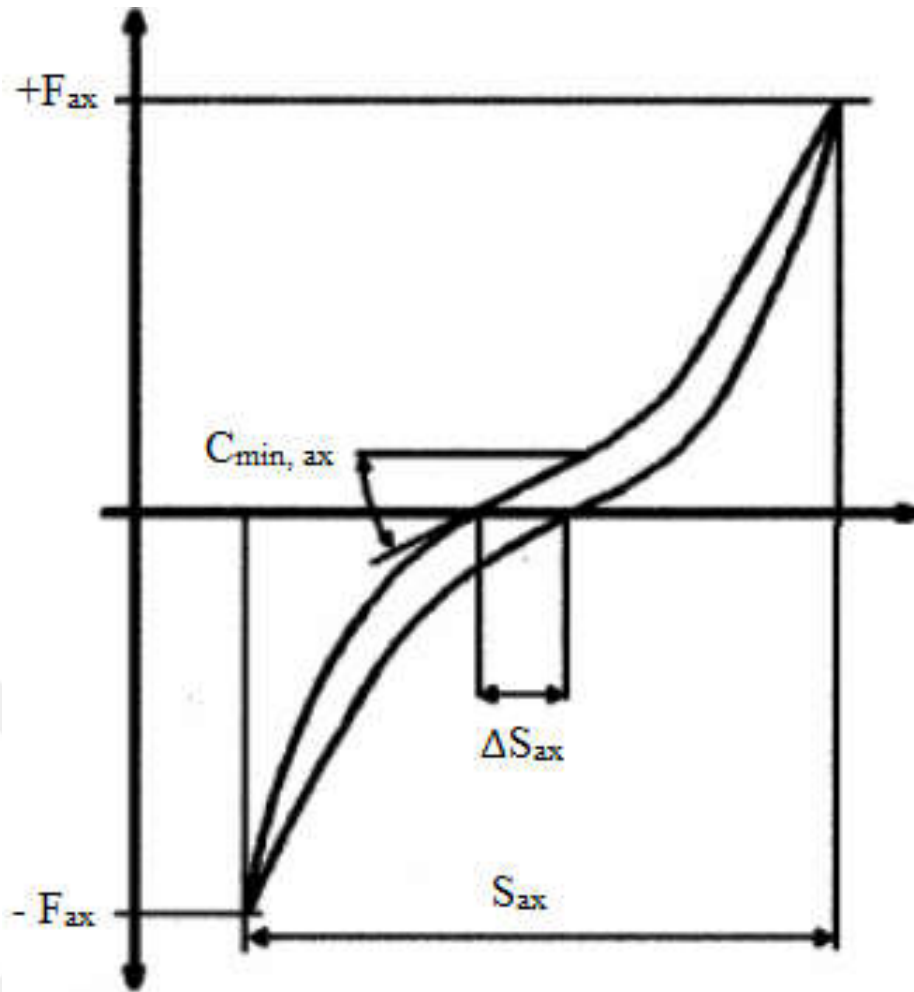


Figure 3.14: Loading of ITR during measurement [9]

The composition of the spring travel  $S_{ax}$  is described schematically in Figure 3.14, which results from the sum of the maximum deflection of the joint in the positive and negative x-direction.

### 3.2.1.3 Stiffness

Stiffness is measured from the curve shown in Figure 3.15 out of Axial Travel measurement. The identifier is given as the smallest tangent gradient  $C_{min,ax}$  of the force-displacement curve. To evaluate the value, two points must be manually placed in the flattest curve section of the force-displacement characteristic. With the help of the tangent, the gradient can be determined. The axial elasticity  $\Delta S_{ax}$  is described as the width of the hysteresis in the force zero crossings and is also shown in Figure 3.15



Value	Description
$+F_{ax}$	axial tensile force
$-F_{ax}$	axial compressive force
$C_{min, ax}$	minimum axial stiffness
$S_{ax}$	axial travel
$\Delta S_{ax}$	axial elasticity

Figure 3.15: Force-Displacement Curve [9]



### 3.2.2 Setting Test

The setting test is performed to evaluate the plastic bearing performance at maximum force and under high temperature.

There are different approaches to determine the forces of automotive steering components during the design, prototype testing, and mass production testing phases.

The first approach is the determination of maximum assist force ( $F_{\max}$ ) by using the path data obtained with the help of strain gauges in test tracks under different conditions [29]. To maintain this approach, production parts and vehicle drive tests are needed.

Second approach; when the steering components are only at design phase, not manufactured and tested yet, it is not possible to get data from the road. The loads on the examined part of the vehicle can be determined at the design stage by using the multi-body dynamics model, [29] which is the second approach to calculate the loads from the route using the ADAMS program [30].

For the definition of the maximum load on the joints, the design-specific exceptional cases must be used, and the forces determined by that  $F_{\max}$ .

During the setting test, the force is applied as a sinusoidal alternating load in the direction of the tie rod axis. Force application is shown in Figure 3.16. During testing, both ball joints are heated up to 80°C by air blow heaters. Setting test rig is shown in Figure 3.17. Complete tie rod assemblies are tested by the axial loading of  $\pm 23$  kN by 3 cycles [9].

The assembly length of inner and outer tie rods is 406.51 mm which is the total length in car steering assembly condition. Acceptance criteria for before and after test is shown in Table 3.3. Criteria is defined according to the standard AK-LH-14.

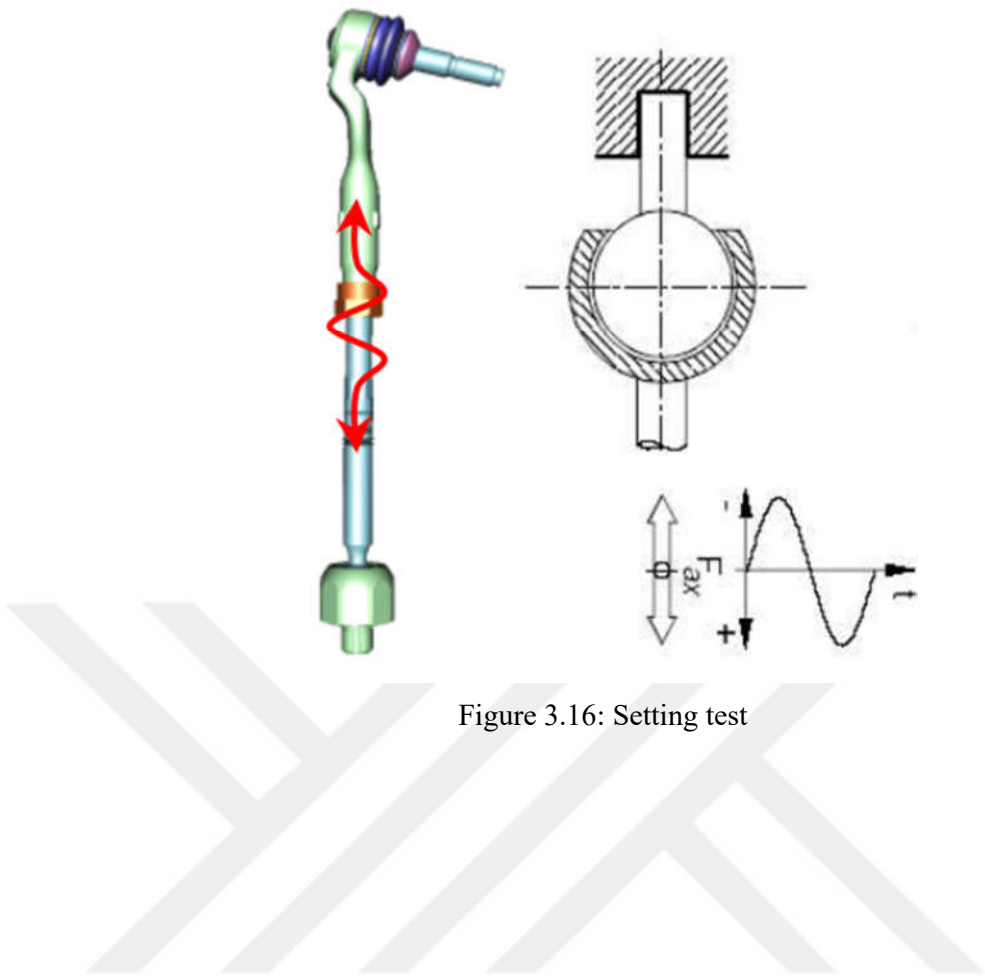


Figure 3.16: Setting test

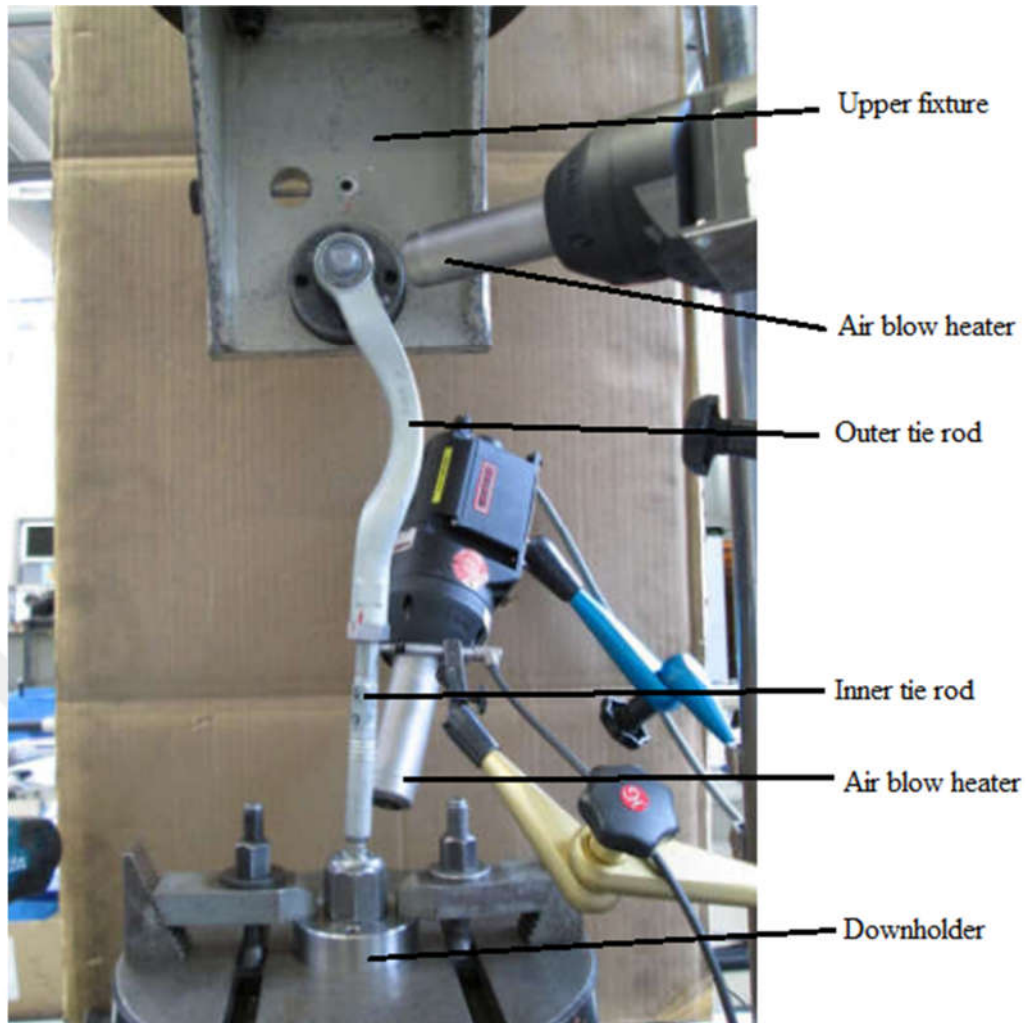


Figure 3.17: Setting Test Rig

Acceptance criteria are as below; [9]

Table 3.3: Setting test acceptance criteria

	Before Testing	After Testing
Articulation torque $M_k$	0.5-3.5 Nm	0.2-3.5 Nm
Axial travel $S_{ax}$	0.05 mm max at $\pm 3$ kN	0.4 mm max at $\pm 3$ kN
Axial stiffness $C_{min,ax}$	100 kN/mm min.	2 kN/mm min.

### 3.2.3 Wear Test

In the wear test, the functional performance of the inner tie rod is investigated after the worn ball race. Definition of load requirements is done in the same way as explained in 3.2.2 Setting Test.

During the wear test, the force is applied in the axial direction of the tie rod. The inner tie rod direction is ensured by fixing the housing on the test rig to apply articulation angle and by clamping the ball stud to apply the axial force. The joint area is heated up to 80°C in heat chamber as test requirement shown in Table 3.4. At high temperatures, POM material is worn more than room temperature [18]. The installation position of the specimen is adjusted as specified on the vehicle. Demonstration of the wear test is shown in Figure 3.18.

Requirements of the testing

- Axial force  $F_{ax}$
- Tilting angle according to specification
- Heating the ball joint to 80°C

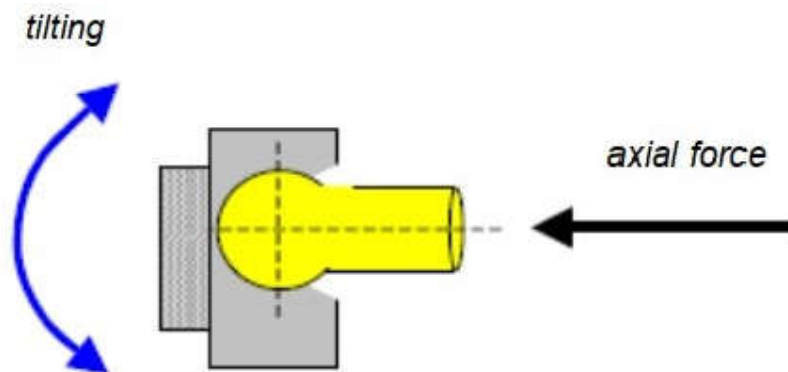


Figure 3.18: Wear test figure [9]

Inner tie rods are tested according to the block cycle defined in Table 3.4 [9]. This block cycle is repeated 8 times for the sample. Wear test rig is shown in Figure 3.19.

Table 3.4: Wear test block cycle

Test Load [kN]	Frequency [Hz]	Articulation Angle [°]	Temperature [°C]	Cycle [LC]
±8884	2	14	80	1250
±7625	4	14	80	2500
±5724	4	14	80	2500
±4464	2	14	80	6250
±3276	1	14	80	25.000
±2468	2	14	80	25.000

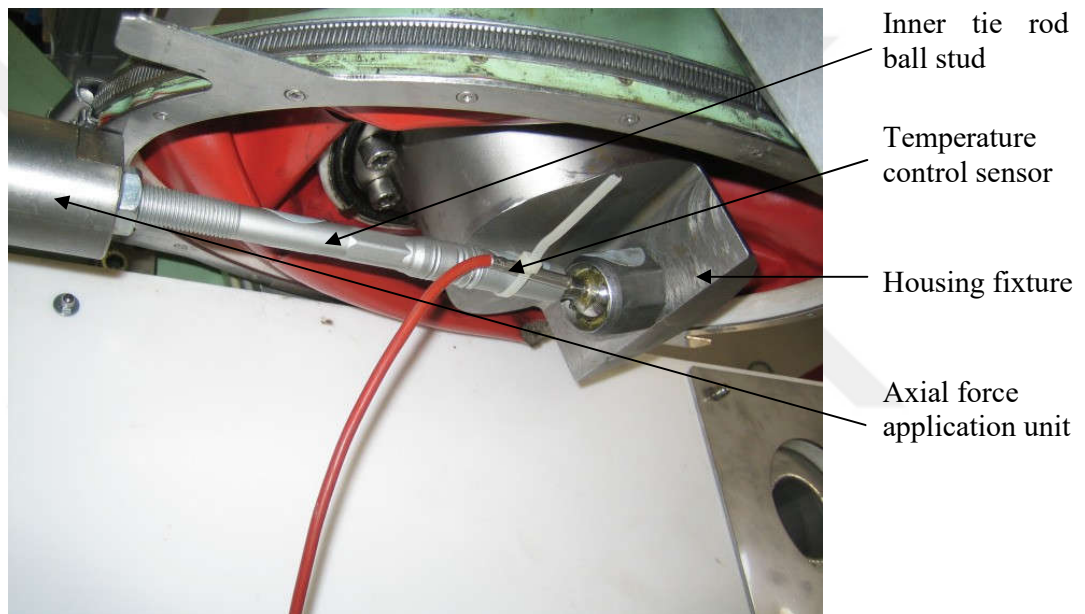


Figure 3.19: Wear Test Rig

Acceptance criteria before and after wear test is shown in Table 3.5. [9]

Table 3.5: Acceptance criteria before and after wear test

	Before Testing	After Testing
Articulation torque $M_k$	0.5-3.5 Nm	0.2-3.5 Nm
Axial travel $S_{ax}$	0.05 mm max at $\pm 3$ kN	0.4 mm max at $\pm 3$ kN
Axial stiffness $C_{min,ax}$	100 kN/mm min.	2 kN/mm min.



# Chapter 4

## Results and Discussions

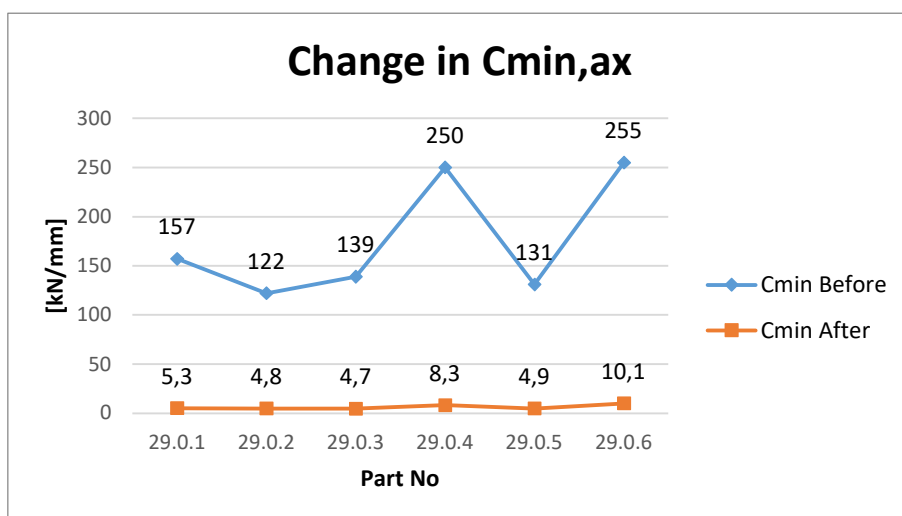
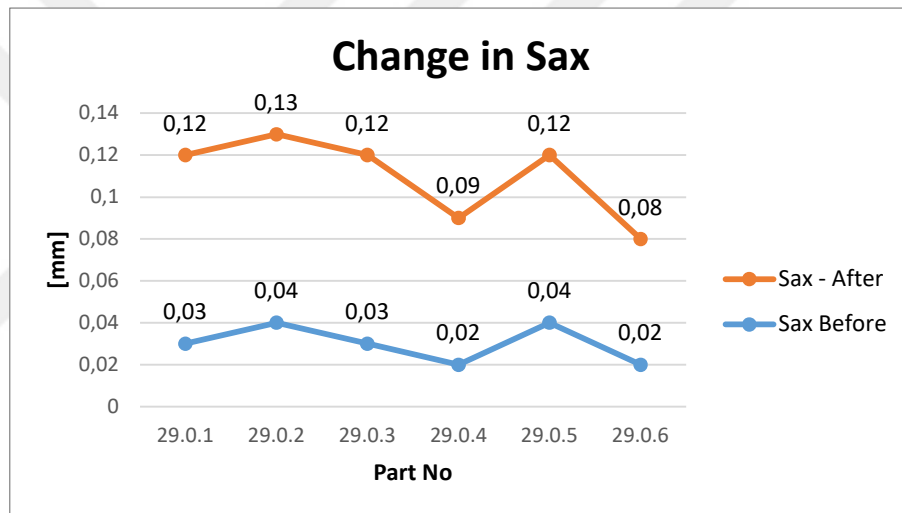
In this section, the experimental results are evaluated. First, the reference sample of Ø29 ball size design results is evaluated. Since Ø29 ball diameter is tested only for reference to the new smaller ball joint production, all functional measurements before and after setting and wear tests are evaluated as acceptable according to defined requirements in respect to AK-LH-14.

### 4.1 Test Results of Ø29 Ball Size Inner Tie Rod

Functional measurements are completed as shown in Figure 3.15. Spring travel  $S_{ax}$ , Stiffness  $C_{min,ax}$ , Articulation torque  $M_k$  are measured and stated in the required range, consequently wear test is performed on samples numbered from 29.0.1 to 29.0.6 according to wear test block cycle shown in Table 3.2. After the wear test, the setting test is performed to samples numbered from 29.0.7 to 29.0.12. All test results are evaluated as acceptable. Results are shown in Table 4.1 and 4.2.

Table 4.1: Batch 0 functional measurements of Ø29 ball size before and after the wear test

Sample No	Before Wear Test			After Wear Test		
	S <sub>ax</sub> [mm]	C <sub>min,ax</sub> [kN/mm]	M <sub>k</sub> [Nm]	S <sub>ax</sub> [mm]	C <sub>min,ax</sub> [kN/mm]	M <sub>k</sub> [Nm]
29.0.1	0,03	157	1,4	0,12	5,3	0,4
29.0.2	0,04	122	1,5	0,13	4,8	0,4
29.0.3	0,03	139	1,3	0,12	4,7	0,4
29.0.4	0,02	250	1,7	0,09	8,3	0,6
29.0.5	0,04	131	1,6	0,12	4,9	0,4
29.0.6	0,02	255	2,1	0,08	10,1	0,6





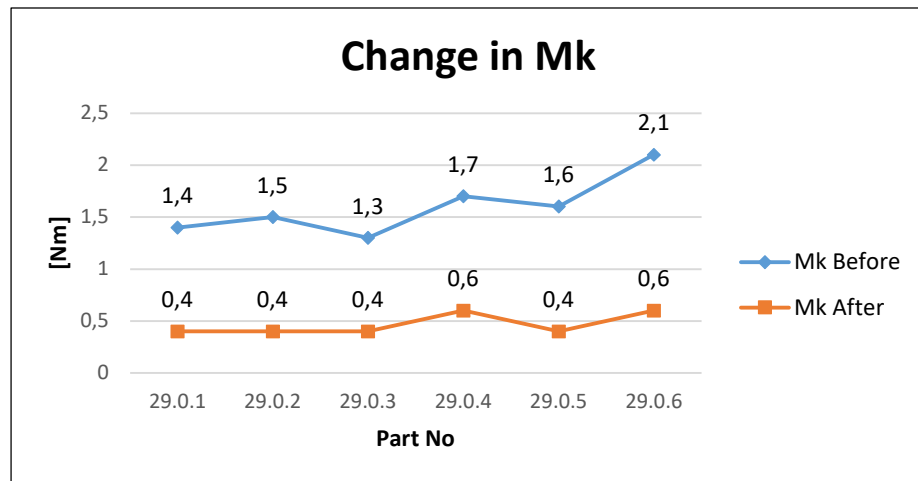


Figure 4.1: Batch 0 change in  $S_{ax}$ ,  $C_{min,ax}$ , and  $M_k$  before and after the wear test

As observed in Table 4.1 and Figure 4.1, after the wear test, functional measurements are repeated and it is seen that there is a significant drop at  $C_{min,ax}$ , and increase at  $S_{ax}$  in comparison to pre-test measurements. This means that because of the wear effect on plastic ball race, ball stud could travel more at the same loading level ( $\pm 3$  kN), and the angle on the force-displacement curve (Figure 3.14) has decreased. On the other hand, measurement results are still in the range of acceptance criteria.

There is also a significant drop in the articulation torque measurement ( $M_k$ ) values. This means that the wear at ball race after testing has also created performance loss at torque. On the other hand, measurement results are still in the range of acceptance criteria.

As observed in Table 4.2 and Figure 4.2 there is a significant drop in  $C_{min,ax}$ ,  $M_k$  and increase in  $S_{ax}$  after setting test in comparison to before setting test measurements. This means that during the setting test, the ball race has been deformed because of high temperature and loading. On the other hand, measurement results are still in the range of acceptance criteria.

Table 4.2: Batch 0 functional measurements of Ø29 ball size before and after the setting test

Sample No	Before Setting Test			After Setting Test		
	S <sub>ax</sub> [mm]	C <sub>min,ax</sub> [kN/mm]	M <sub>k</sub> [Nm]	S <sub>ax</sub> [mm]	C <sub>min,ax</sub> [kN/mm]	M <sub>k</sub> [Nm]
29.0.7	0,02	150	1,4	0,15	7,6	1,1
29.0.8	0,03	130	1,4	0,16	4,6	1,0
29.0.9	0,04	128	1,9	0,16	5,5	0,9
29.0.10	0,02	210	1,4	0,17	4,2	0,9
29.0.11	0,03	145	1,6	0,15	6,3	1,0
29.0.12	0,02	226	1,4	0,18	4,5	0,9



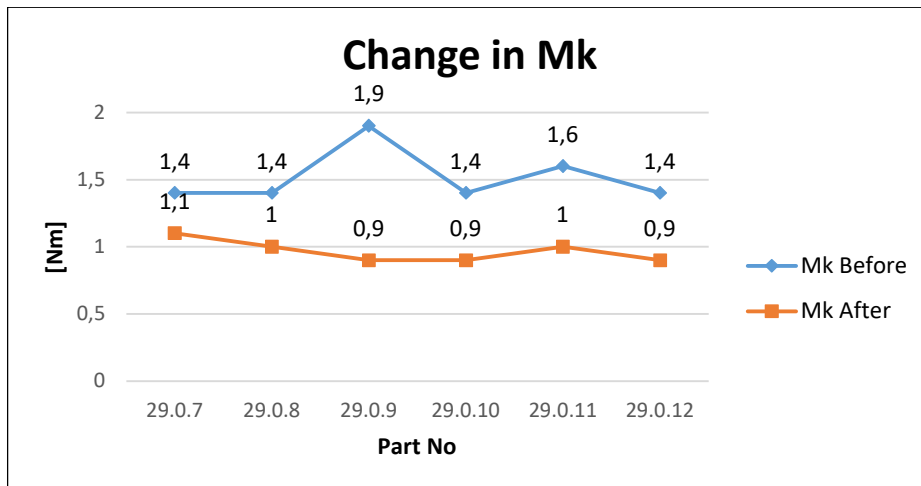
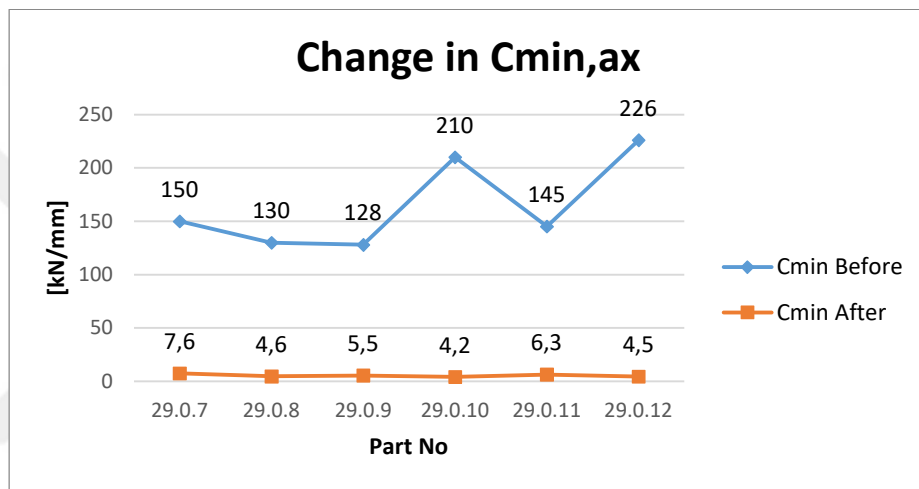
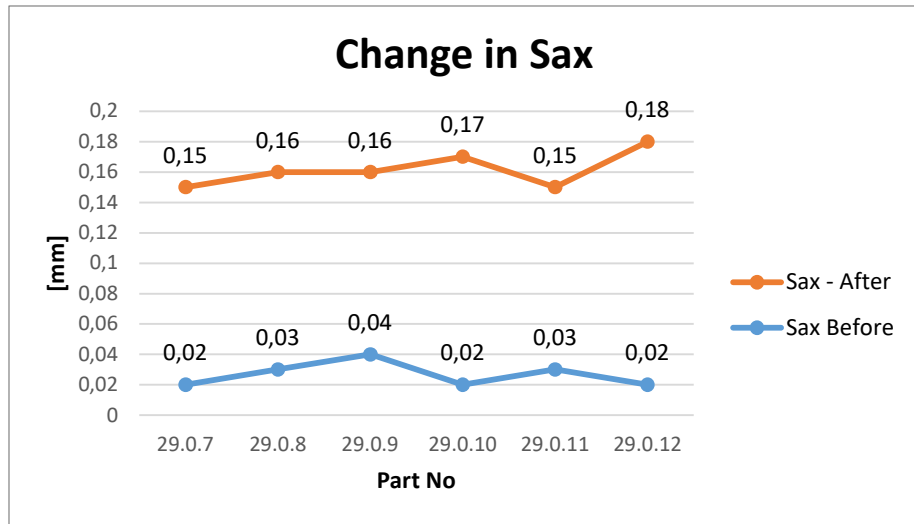


Figure 4.2: Batch 0 change in  $S_{ax}$ ,  $C_{min,ax}$ , and  $M_k$  before and after the setting test

As shown in Figures 4.1 and 4.2, Ø29 ball size is safe to use and fulfill the requirements defined in automotive standard AK-LH-14. In this study, it is targeted to reduce the ball diameter size which can also fulfill the requirements.



## 4.2 New Small Diameter Axial Bearing Design

As stated in Section 4.1 the requirements of AK-LH-14 can be fulfilled with Ø29 ball size. An innovative approach is to fulfill the same requirements with a smaller ball size which will lead to less weight, less volume, less energy and thus lower cost.

### 4.2.1 Oven Tempering Test Results

When the geometry of the ball stud and housing are determined and produced according to the Ø26 ball size, the variants shown in Table 3.2 are tested.

Functional values of the samples are determined before and after testing. Requirements are considered according to Table 3.3 for setting test and Table 3.5 for wear test.

**For Batch 1** of test samples, production is done with “min press force +20 kN” pressing force for pressing operation. Inner tie rods are tempered in the oven at the initial temperature.

Red colored cells show unacceptable results.

Table 4.3: Batch 1 functional measurements of Ø26 ball size before and after the setting test

Sample No	Before Setting Test			After Setting Test			Evaluation
	S <sub>ax</sub> [mm]	C <sub>min,ax</sub> [kN/mm]	M <sub>k</sub> [Nm]	S <sub>ax</sub> [mm]	C <sub>min,ax</sub> [kN/mm]	M <sub>k</sub> [Nm]	
26.1.1	0,02	229	3,9	0,23	6,3	0,7	NOT OK
26.1.2	0,03	197	3,5	0,22	6,6	0,6	OK
26.1.3	0,02	264	3,3	0,23	6,3	0,6	OK
26.1.4	0,02	229	2,8	0,27	4,8	0,5	OK
26.1.5	0,02	230	3,8	0,24	5,5	0,6	NOT OK
26.1.6	0,02	269	3,7	0,22	6,5	0,5	NOT OK

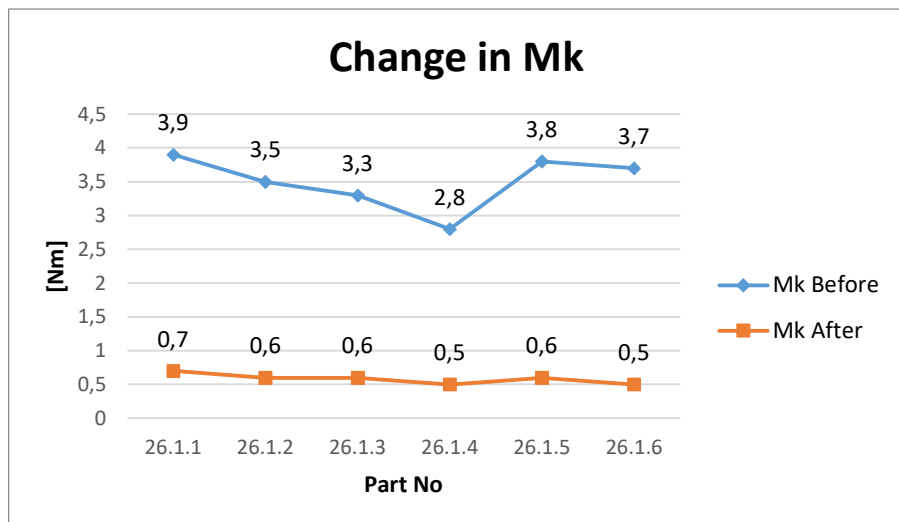
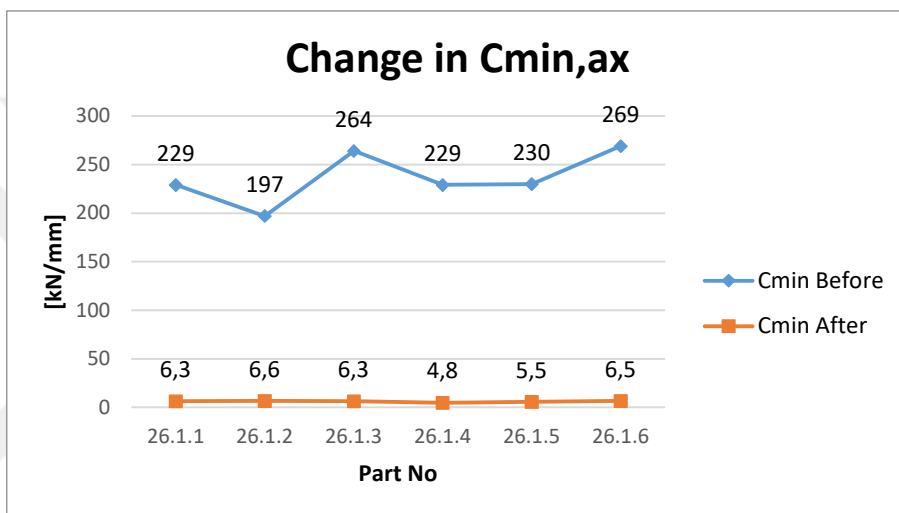
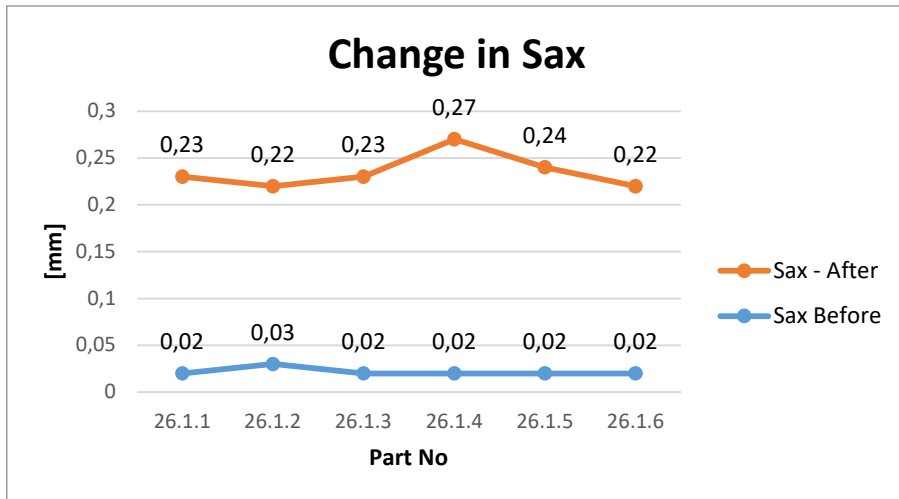


Figure 4.3: Batch 1 change in  $S_{ax}$ ,  $C_{min,ax}$ , and  $M_k$  before and after the setting test

According to the results above, sample numbers 26.1.1, 26.1.5, and 26.1.6 did not fulfill the requirement of  $M_k$  before setting test (red colored cells). Inner tie rods were tested only for information and samples fulfill the requirement after the test. However, because of unacceptable results before the test, samples are evaluated as unacceptable. Also, a wear test is not performed on these samples.

In a conclusion, either press force “min press force +20 kN” is high or tempering temperature is not high enough to ensure acceptable torque results before testing.

Then **Batch 2** is tested. Press force “min press force +20 kN” is applied again, tempering temperature is increased by 10°C to ensure the pre-test measurements for  $M_k$  to be acceptable. Higher tempering temperature can adjust the  $M_k$  to decrease. [18]

Table 4.4: Batch 2 functional measurements of Ø26 ball size before and after the wear test

Sample No	Before Wear Test			After Wear Test			Evaluation
	$S_{ax}$ [mm]	$C_{min,ax}$ [kN/mm]	$M_k$ [Nm]	$S_{ax}$ [mm]	$C_{min,ax}$ [kN/mm]	$M_k$ [Nm]	
26.2.1	0,03	172	3,5	0,07	22	1,1	OK
26.2.2	0,03	150	3,1	0,07	31	0,8	OK
26.2.3	0,03	165	3,1	0,06	30	0,9	OK
26.2.4	0,02	181	3,0	0,06	42	1,1	OK
26.2.5	0,02	199	3,2	0,06	46	1,1	OK
26.2.6	0,03	187	3,2	0,06	54	1,4	OK

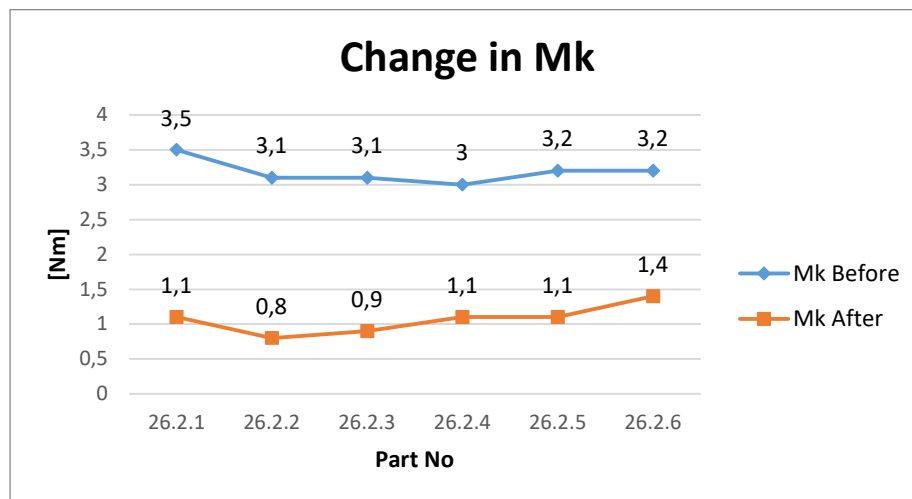
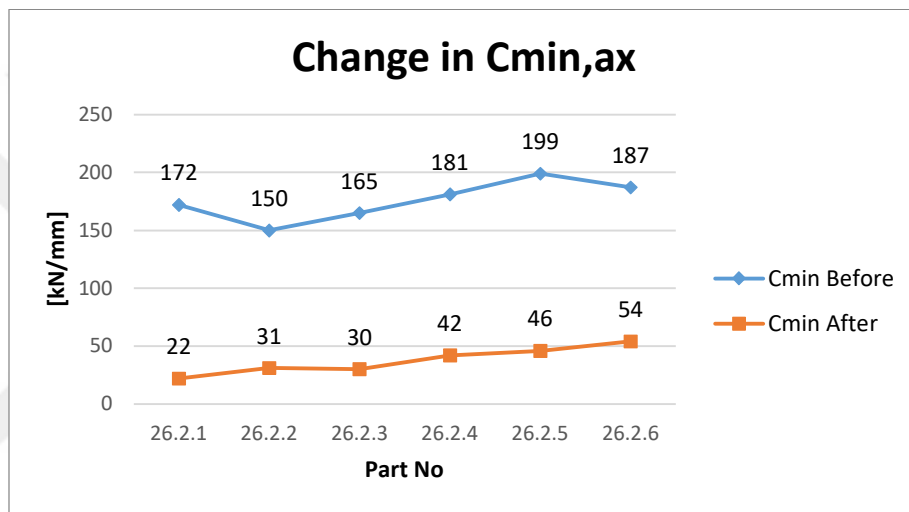
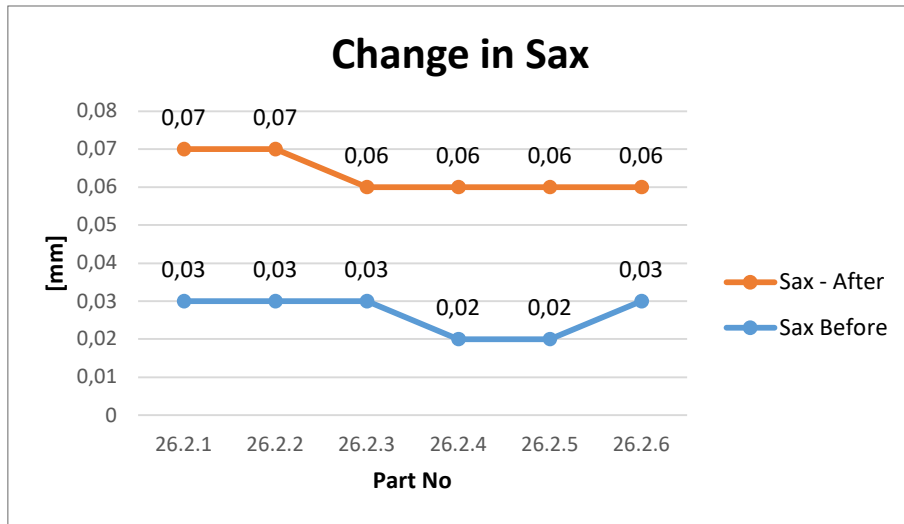


Figure 4.4: Batch 2 change in  $S_{ax}$ ,  $C_{min,ax}$ , and  $M_k$  before and after the wear test



Table 4.5: Batch 2 functional measurements of Ø26 ball size before and after the setting test

Sample No	Before Setting Test			After Setting Test			Evaluation
	S <sub>ax</sub> [mm]	C <sub>min,ax</sub> [kN/mm]	M <sub>k</sub> [Nm]	S <sub>ax</sub> [mm]	C <sub>min,ax</sub> [kN/mm]	M <sub>k</sub> [Nm]	
26.2.7	0,03	187	3,5	0,39	2,4	0,3	OK
26.2.8	0,03	191	3,5	0,35	2,7	0,5	OK
26.2.9	0,03	177	3,1	0,28	3,3	0,4	OK
26.2.10	0,03	195	3,5	0,32	3,4	0,5	OK
26.2.11	0,03	207	3,3	0,29	3,1	0,4	OK
26.2.12	0,03	179	3,5	0,30	3,5	0,5	OK

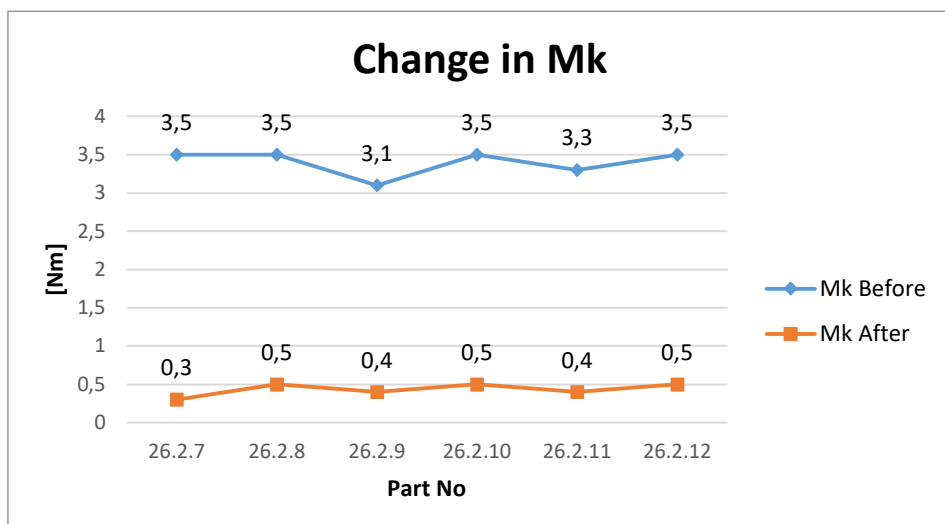
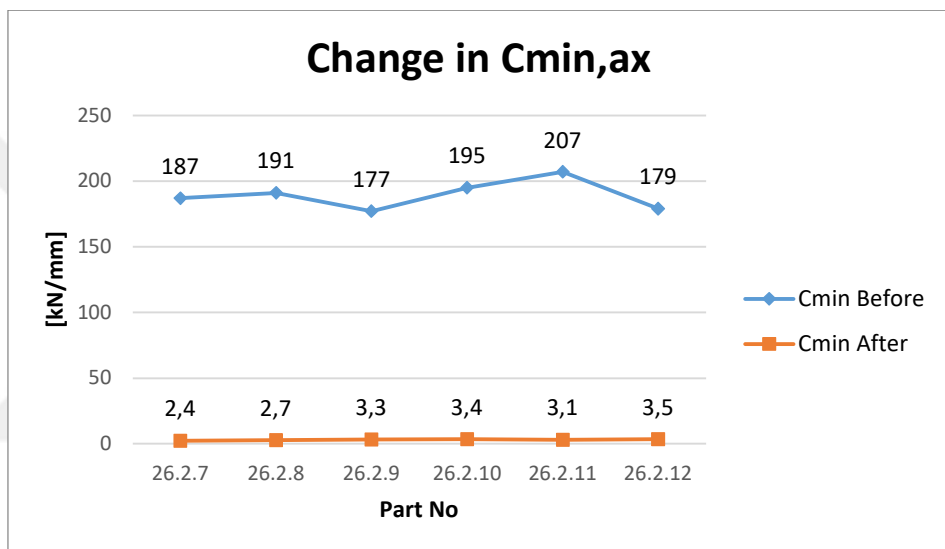
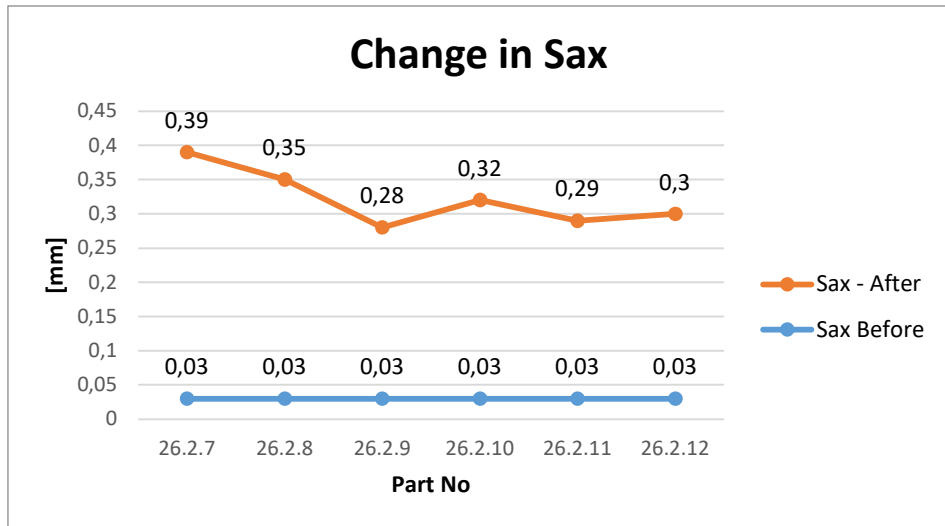


Figure 4.5: Batch 2 change in  $S_{ax}$ ,  $C_{min,ax}$ , and  $M_k$  before and after the setting test

According to pre-test measurements of the wear test, it is evident that torque measurement results are still close to the upper limit but decreased in respect to the **Batch 1** results. This means that a 10°C tempering temperature increase is decreasing the torque to the required level by keeping the pressing force constant.

Evaluation after wear test is also acceptable according to functional measurement results.

Setting test pre-and post-test measurement results are also evaluated as acceptable.

In a conclusion, for Ø26 ball joint production parameters; “min press force +20 kN” press force, Initial +10°C oven tempering temperature fulfills the requirements defined according to AK-LH-14 and can be used for series production.

## 4.2.2 Ball Tempering Test Results

After the first results stated for oven tempering, **Batch 3** is tested which was tempered at the ball area. Assembly is done by using Min press force and the tempering method has been updated to ball tempering.

Table 4.6: Batch 3 functional measurements of Ø26 ball size before and after the wear test

Sample No	Before Wear Test			After Wear Test			Evaluation
	S <sub>ax</sub> [mm]	C <sub>min,ax</sub> [kN/mm]	M <sub>k</sub> [Nm]	S <sub>ax</sub> [mm]	C <sub>min,ax</sub> [kN/mm]	M <sub>k</sub> [Nm]	
26.3.1	0,03	137	1,3	0,07	50	0,6	OK
26.3.2	0,03	156	0,8	0,07	47	0,5	OK
26.3.3	0,03	201	1,2	0,05	80	1,0	OK
26.3.4	0,03	167	0,9	0,06	55	0,6	OK
26.3.5	0,03	195	1,1	0,05	76	1,2	OK
26.3.6	0,02	225	1,2	0,05	94	1,2	OK

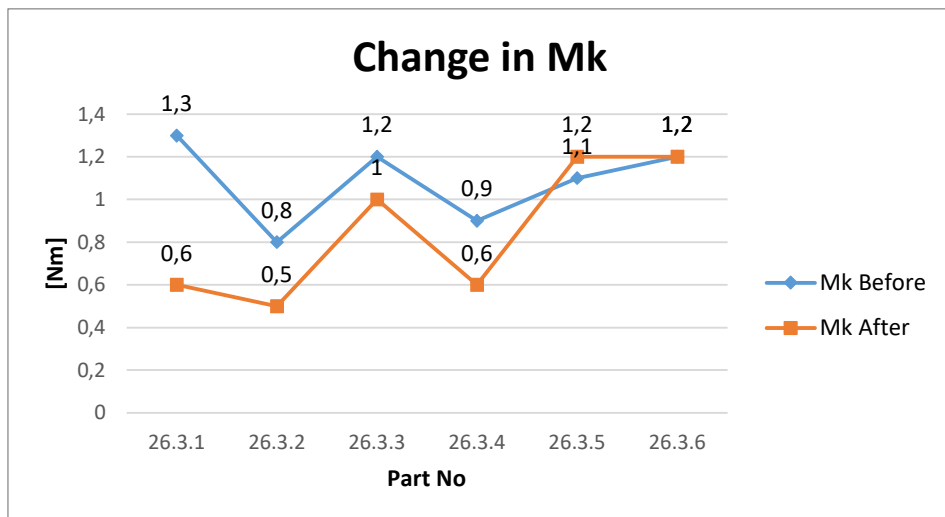
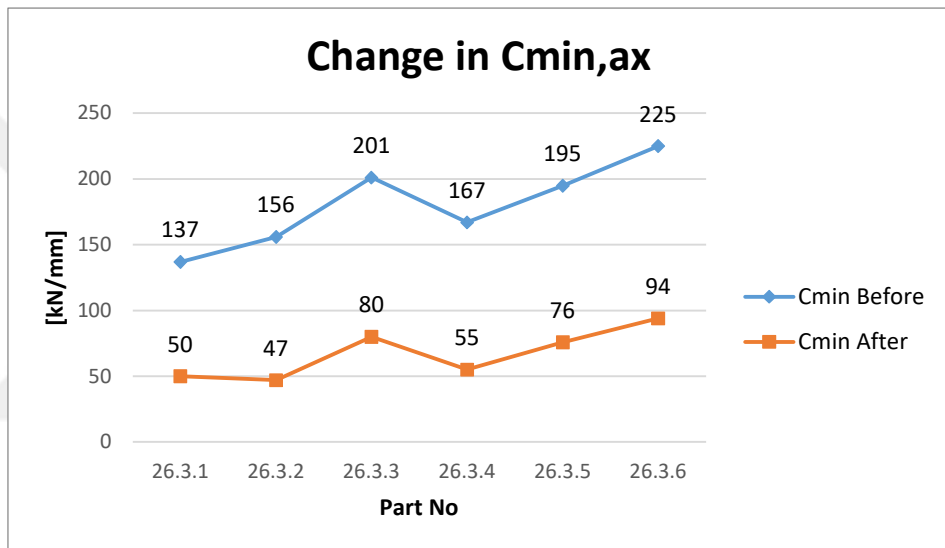
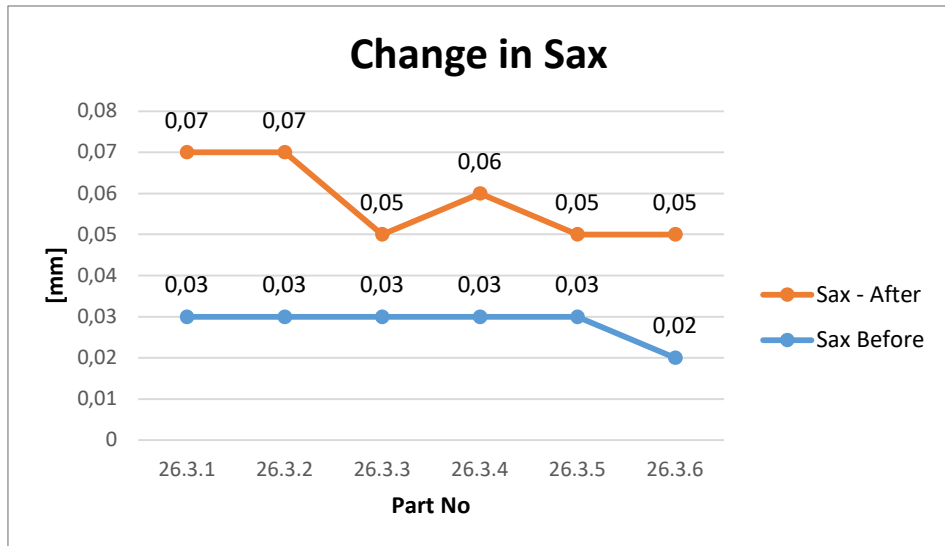


Figure 4.6: Batch 3 change in  $S_{ax}$ ,  $C_{min,ax}$ , and  $M_k$  before and after the wear test

Table 4.7: Batch 3 functional measurements of Ø26 ball size before and after the setting test

Sample No	Before Setting Test			After Setting Test			Evaluation
	S <sub>ax</sub> [mm]	C <sub>min,ax</sub> [kN/mm]	M <sub>k</sub> [Nm]	S <sub>ax</sub> [mm]	C <sub>min,ax</sub> [kN/mm]	M <sub>k</sub> [Nm]	
26.3.7	0,03	152	1,1	0,44	1,7	0,4	NOT OK
26.3.8	0,03	183	1,1	0,18	5,1	0,4	OK
26.3.9	0,03	156	1,0	0,49	1,7	0,4	NOT OK
26.3.10	0,03	171	1,1	0,44	1,9	0,3	NOT OK
26.3.11	0,03	171	1,2	0,45	1,9	0,3	NOT OK
26.3.12	0,03	187	1,4	0,47	1,7	0,3	NOT OK

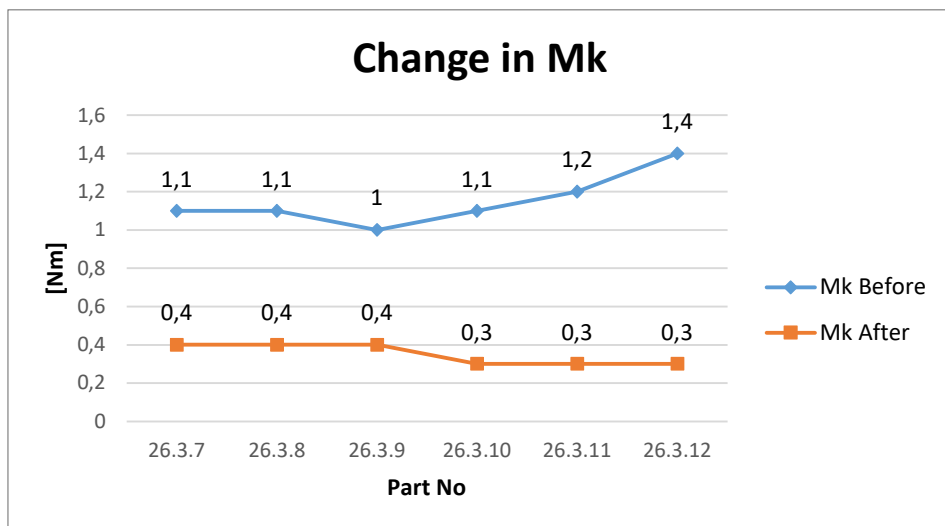
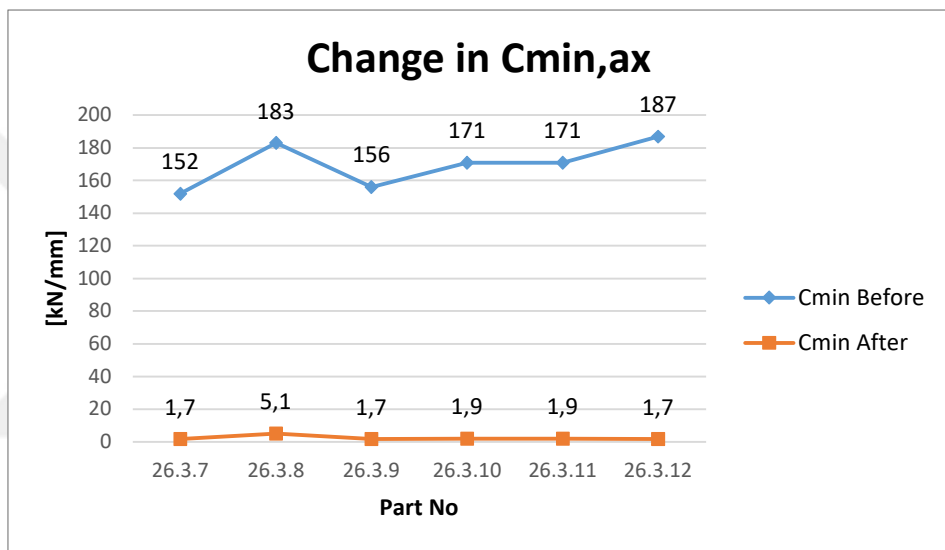
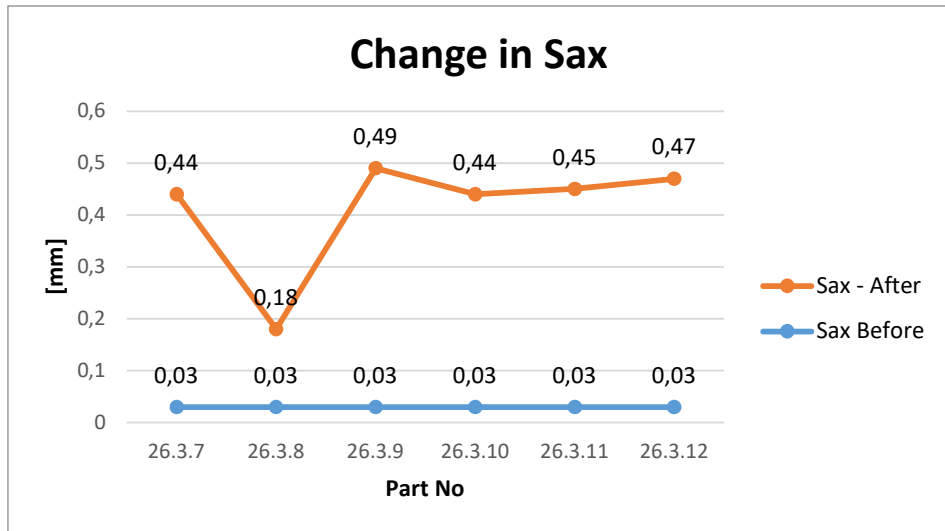


Figure 4.7: Batch 3 change in  $S_{ax}$ ,  $C_{min,ax}$ , and  $M_k$  before and after the setting test

According to the results above, pre and post measurements of the wear test fulfills the requirements. Usage of lower press force decreased the inner stress at ball joint which resulted in acceptable measurement values of  $M_k$ .

On the other hand, pre-test measurements of setting test were evaluated as acceptable. After testing, axial travel  $S_{ax}$  has increased more than the allowed limit and in respect to  $S_{ax}$  measurements stiffness  $C_{min,ax}$  has decreased more than the allowed limit. 5 out of 6 samples are evaluated as unacceptable.

This means that a reduction in press force decreased the pre-torque performance inside the requirement. Also, after the wear test, all functional values are within the limit because wear on the ball race was within allowed limits.

However, deformation on ball race after setting test caused unacceptable results at  $S_{ax}$  and  $C_{min,ax}$ . The travel of the ball stud inside the joint is more than allowed. In a conclusion, Min press force is not enough to ensure a safe design.

For the final test trials **Batch 4** is tested concerning the **Batch 3** results. The outcome from **Batch 3** results showed that Min press force is not enough to fulfill the requirements according to AK-LH-14. For increased performance and acceptable evaluation, press force has been increased to Min press force + 10 kN.

According to pre-test measurements of wear test, results are in the middle range of the requirement. This means that increase in press force is also increasing the pre-test torque results.

Evaluation after wear test is also acceptable according to functional measurement results.

Setting test pre-and post-test measurement results are also evaluated as acceptable.

In a conclusion, for Ø26 ball joint production parameters; Min press force + 10 kN, initial ball tempering temperature fulfills the requirements defined according to AK-LH-14 and can be used for series production.

Table 4.8: Batch 4 functional measurements of Ø26 ball size before and after the wear test

Sample No	Before Wear Test			After Wear Test			Evaluation
	S <sub>ax</sub> [mm]	C <sub>min,ax</sub> [kN/mm]	M <sub>k</sub> [Nm]	S <sub>ax</sub> [mm]	C <sub>min,ax</sub> [kN/mm]	M <sub>k</sub> [Nm]	
26.4.1	0,02	273	2,1	0,04	135	1,7	OK
26.4.2	0,02	235	2,2	0,04	125	1,8	OK
26.4.3	0,02	235	2,1	0,04	109	1,5	OK
26.4.4	0,02	276	2,0	0,04	135	1,5	OK
26.4.5	0,02	293	2,1	0,04	102	1,2	OK
26.4.6	0,02	228	1,9	0,05	93	1,3	OK





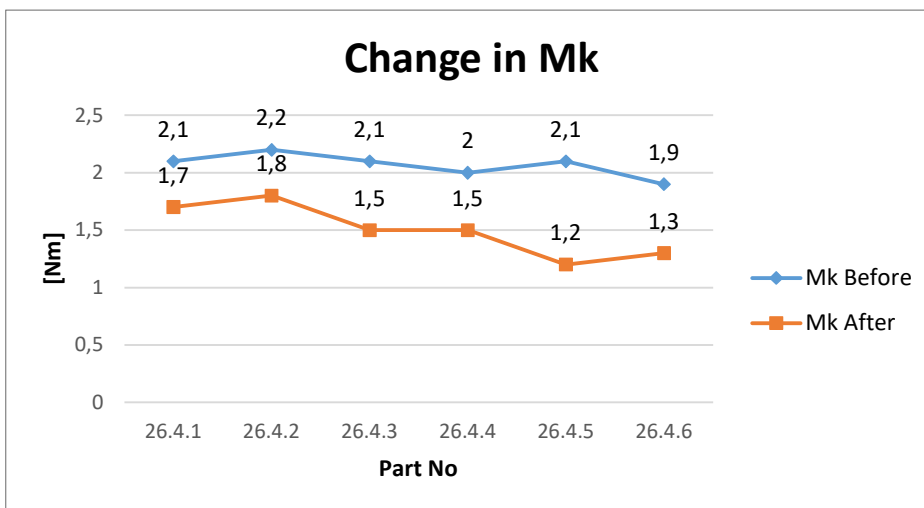
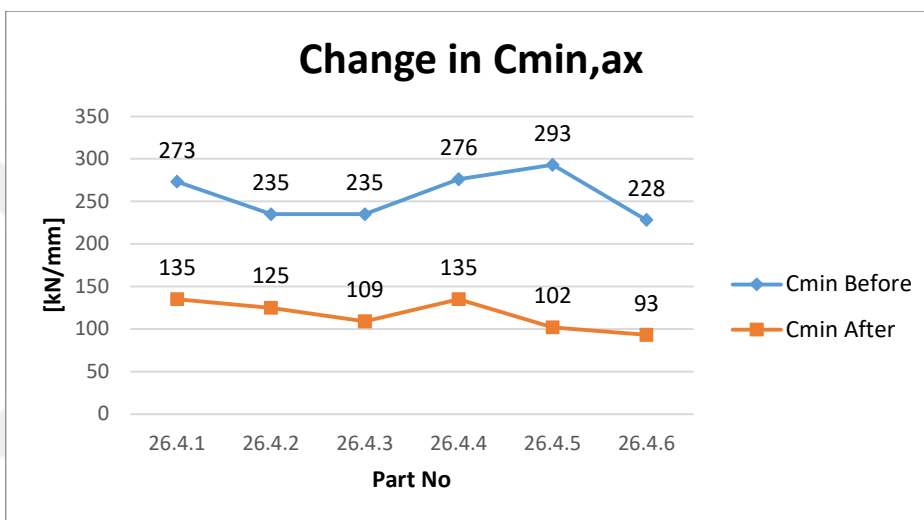
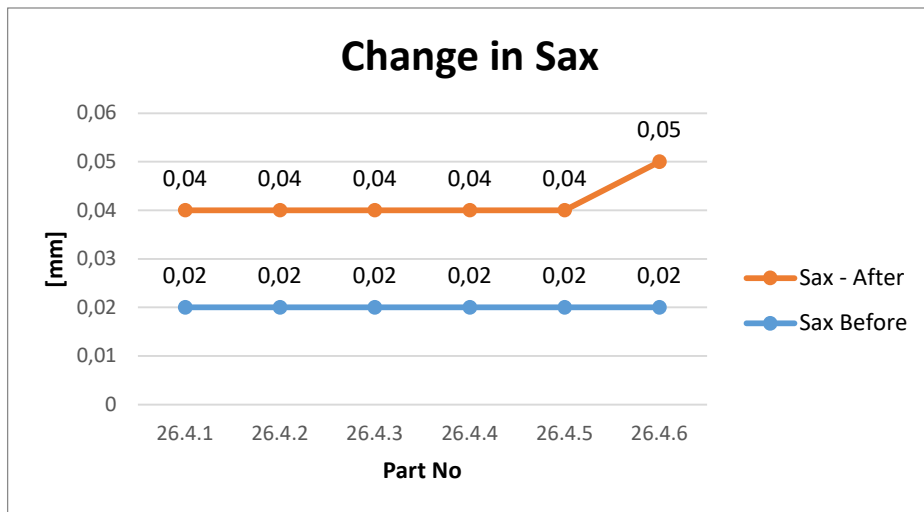


Figure 4.8: Batch 4 change in  $S_{ax}$ ,  $C_{min,ax}$ , and  $M_k$  before and after the wear test

Table 4.9: Batch 4 functional measurements of Ø26 ball size before and after the setting test

Sample No	Before Setting Test			After Setting Test			Evaluation
	S <sub>ax</sub> [mm]	C <sub>min,ax</sub> [kN/mm]	M <sub>k</sub> [Nm]	S <sub>ax</sub> [mm]	C <sub>min,ax</sub> [kN/mm]	M <sub>k</sub> [Nm]	
26.4.7	0,02	242	2,4	0,15	6,5	0,6	OK
26.4.8	0,02	253	1,8	0,13	6,2	0,4	OK
26.4.9	0,02	267	2,0	0,12	7,1	0,6	OK
26.4.10	0,02	242	2,3	0,11	7,3	0,5	OK
26.4.11	0,02	222	2,0	0,11	7,8	0,5	OK
26.4.12	0,02	250	2,3	0,14	7,7	0,5	OK



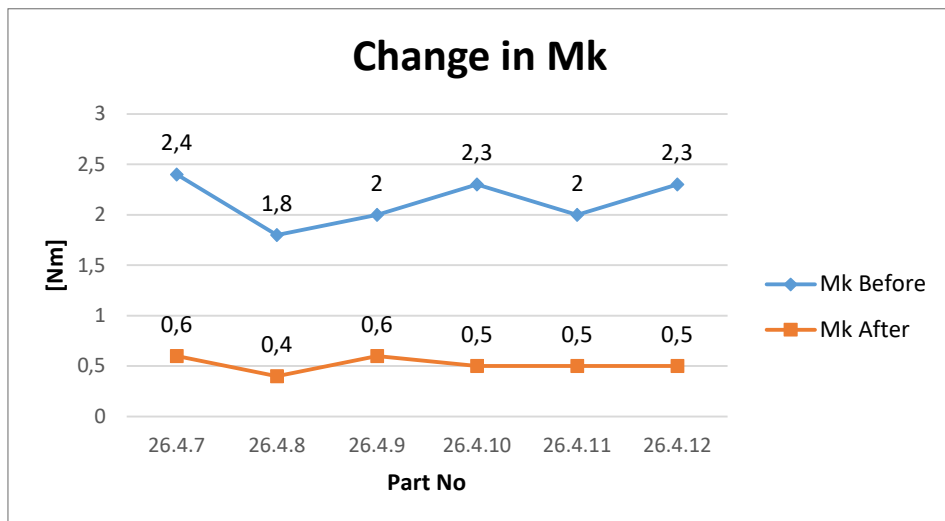
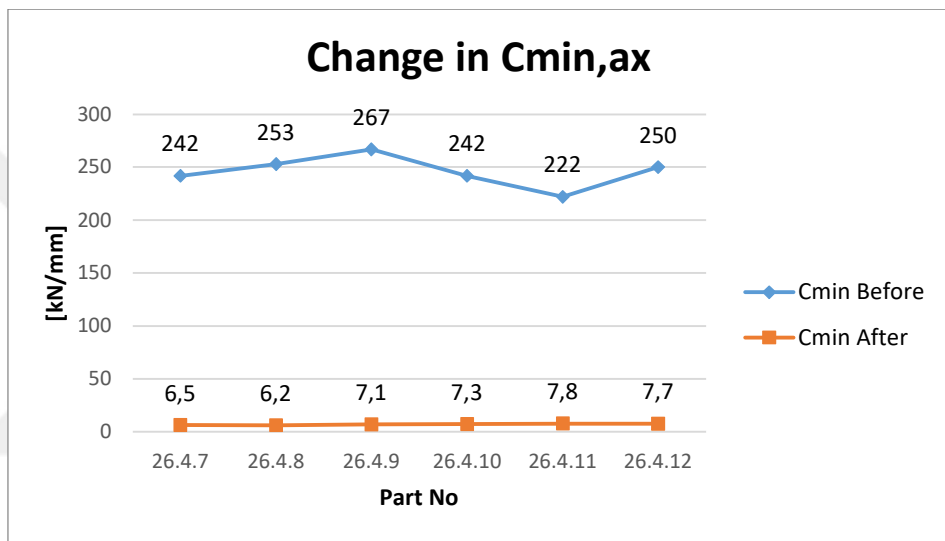
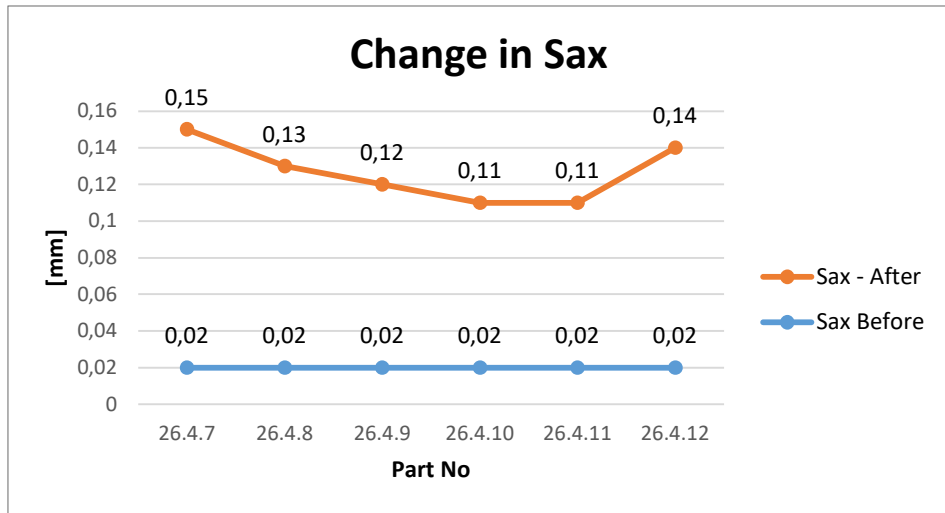


Figure 4.9: Batch 4 change in  $S_{ax}$ ,  $C_{min,ax}$ , and  $M_k$  before and after the setting test

At the end of the study, 2 different production and assembly parameter values are determined for series production.



# Conclusion

In this study, a smaller diameter plastic bearing was designed and manufactured instead of the relatively large diameter plastic bearing, which is still in use. Thus, it is aimed to lighten the product and reduce its cost.

The functional values specified by the current standards and the products have been determined.

The new Ø26 ball diameter inner tie rod samples were assembled in 3 different groups with different assembly force, tempering type and tempering temperatures.

All variations of all three groups were tested for their functional performance and the best 4 variations were selected for wear and setting.

The test samples are tested in the wear test device at the loading of the road simulating conditions. All samples were subjected to wear test under load, simulating road conditions in the test device.

Functional values were measured both before and after the setting test, and the results were compared, as was done in the wear test.

For **Batch 1**, only the setting test was performed because the articulation torque in three parts exceeded the allowable range of 0.5 - 3.5 Nm with the values 3.9, 3.8, 3.7 Nm. Although functional measurements obtained after the setting test were within the expected range, the results before the test were out of range, as a result of the evaluation, it was determined that the tempering temperature should be increased and the wear test was not continued.

For **Batch 2**, tempering temperature was increased by 10 ° C and functional values were measured. As all functional measurements before tests are within the specified range, wear and setting tests have been carried out for this batch. Since the values

obtained after the tests meet the acceptance criteria, this batch has been evaluated as having suitable assembly parameters for series production.

For **Batch 3**, the tempering method was ball tempering instead of oven tempering. In the measurements before the test, all samples were evaluated as in the range of acceptance criteria. Wear tests and setting tests were carried out. After the wear tests, functional values were measured again, and it was seen that all values met the acceptance criteria. After the setting tests, five out of six pieces could not meet the axial displacement and stiffness criteria. This occurred because of excessive wear of the plastic bearing and it was decided that the press force during assembly should be increased.

The **Batch 4** samples are again assembled by ball tempering and with 10 kN more press force than batch samples. According to the measurements made, it has been observed that the functional values of all parts before the test are within the acceptance criteria and the tests can be continued. Since functional values meet the acceptance criteria after the wear and setting tests, this batch has been evaluated as having the appropriate assembly parameters for series production.

As a result of the study, the production methods of the **Batch 2** and **Batch 4** samples were determined as appropriate for series production. In both batches, reduction of around 10% in weight and reduction of around 8% in costs were achieved. In this case both **Batch 2** and **Batch 4** are preferred for serial production according to tempering method. If oven tempering will be performed then **Batch 2** is preferred, if ball tempering will be performed then **Batch 4** is preferred.

In the later studies, a new plastic bearing design with a lower diameter can be realized by performing tests with different plastic bearing materials.

# References

- [1] Heiβing B, Ersoy M. Chassis Handbook. 1st Edition. Wiesbaden: Vieweg+Teubner; 2011.
- [2] Sarıkaya A. Güç Takviyeli Direksiyon Sistemlerinin Modellenmesi Ve Kontrolü (master's thesis). İstanbul Technical University, Institute of Science and Technology, 2007. <https://tez.yok.gov.tr/>
- [3] Ünal, F., Elektrikli Direksiyon Sistemi, (master's thesis). İstanbul Technical University, Institute of Science and Technology, 2007. <https://tez.yok.gov.tr/>
- [4] Tas, K. Experimental and Numerical Analysis of Passenger Car Tie Rod Push-Out and Fatigue Performance (master's thesis). Izmir: Ege University, 2017. <https://tez.yok.gov.tr/>
- [5] Gürsel, K.T., ve Çalır, S., Sıvama ile Monte Edilen Mekanizmalarda Oluşan Sıkıştırma Kuvvetlerinin Saptanması. Mühendislik Bilimleri Dergisi, Pamukkale Üniversitesi 2011; 17 (3): 143-156
- [6] Şener A.Ş., Araç yorulma ömürlerinin sonlu elemanlar yöntemi ile belirlenmesi, Taşıt Teknolojileri Elektronik Dergisi 2010; 2 (3): 13-28.
- [7] Falah, A.H., Alfares, M.A and Elkholy, A.H., Failure Investigation of a Tie Rod End of an Automobile Steering System, Engineering Failure Analysis 2007; 14 (5): 895-902. [doi.org/10.1016/j.engfailanal.2006.11.045](https://doi.org/10.1016/j.engfailanal.2006.11.045)
- [8] Essienubong, I. A., Ikechukwu, O., Ebunilo, P. O., Ikpe, E. E., Static analysis on a vehicle tie rod to determine the resulting buckling displacement, International Journal of Industrial and Manufacturing Systems Engineering, 2016; 1(1): 16-24. [doi.org/10.11648/j.ijimse.20160101.13](https://doi.org/10.11648/j.ijimse.20160101.13)
- [9] AK-LH 14 Suspension Joints/Requirements and Testing. Working Committee Specification Book; 2004

- [10] Pehlivan, M. K. ve Özsoy, M.. Rot başının bilgisayar destekli yapısal çözümlenmesi. Bilecik Şeyh Edebali Üniversitesi Fen Bilimleri Dergisi 2014; 1(1): 1-7.
- [11] Shende, A. and Padole, V., , Failure Analysis and Fatigue Life Improvement of Modified Steering Mechanism (Tie-Rod) of Heavy Commercial Vehicles using FEA, International Journal for Scientific Research&Development 2016; 4(07): 283-284
- [12] Flores P., Ambrosio J., Claro J.C.P., Lankarini H.M., Koshy C.S., A study on Dynamics of mechanical systems including joints with clearance and lubrication, Mechanism and Machine Theory 2006; 41 (3): 247-261. doi.org/10.1016/j.mechmachtheory.2005.10.002
- [13] Zhao B., Zhang Z., Dai X., Prediction of wear at revolute clearance joints in flexible mechanical systems, Malaysian International Tribology Conference 68, 2013, 661-667. doi.org/10.1016/j.proeng.2013.12.236
- [14] Mohamed E., Yusuff M. Wahab D., Application of rain flow cycle counting in the reliability prediction of automotive front corner module system, IEEE, 2009. doi.org/10.1109/ICIEEM.2009.5344498
- [15] Köhne, T., Investigation of the possible uses of fiber-reinforced plastic shells for ball joints to increase the load capacity and the permissible temperature range; Dielingen: 1995
- [16] M. J. Neale The Tribology Handbook. 2<sup>nd</sup> ed.: Butterworth Heinemann; 2001
- [17] Tribologie, Reibung und Verschleiß (Grundlagen) [Internet] <https://docplayer.org/20745410-3-1-tribologie-reibung-und-verschleiss-grundlagen.html> (Erişim 02.04.2021)
- [18] Bergmann, W., Werkstofftechnik, Part 2: Application, Carl Hanser Verlag; 1987



- [19] Homepage of BASF [Internet] [http://www.plasticsportal.net/wa/EU~de\\_DE/Catalog/ePlastics/doc/BASF/production/ultraform/mechanical\\_properties\\_ultraform.xdoc](http://www.plasticsportal.net/wa/EU~de_DE/Catalog/ePlastics/doc/BASF/production/ultraform/mechanical_properties_ultraform.xdoc) (Erişim 02.04.2021)
- [20] Schwarz, O. Kunststoffkunde, 2nd Edition, Vogel Buchverlag; 1988
- [21] Homepage of TU-Darmstadt [Internet] [http://elib.tu-darmstadt.de/diss/000534/Dissertation\\_Kapitel\\_1\\_bis\\_2.pdf](http://elib.tu-darmstadt.de/diss/000534/Dissertation_Kapitel_1_bis_2.pdf) (Erişim 02.04.2021)
- [22] H. Unal, U. Sen, A. Mimaroglu Friction and wear behaviour of unfilled engineering thermoplastic. *Materials & Design*. Elsevier; 2003; 24 (3): 183-187 [doi.org/10.1016/S0261-3069\(03\)00018-9](https://doi.org/10.1016/S0261-3069(03)00018-9)
- [23] Jinyao Chen, Ya Cao, Huilin Li, Investigation of the friction and wear behaviors of polyoxymethylene/linear low-density polyethylene/ethylene-acrylic-acid blends; 2006; 260 (11–12): 1342-1348. [doi.org/10.1016/j.wear.2005.09.035](https://doi.org/10.1016/j.wear.2005.09.035)
- [24] Unal H, Sen U, Mimaroglu A. Abrasive wear behaviour of polymeric materials. *Materials & Design*; 2005; 26 (8): 705-710. [doi.org/10.1016/j.matdes.2004.09.004](https://doi.org/10.1016/j.matdes.2004.09.004)
- [25] Kırılı, O. Determining Mechanical Properties of the Steering Joint Ball Race Material Acetal/POM at Comperisson Loading and Different Temperatures with Experimental and Numeric Simulation (doctoral thesis). Ege University Izmir; 2009.
- [26] Gao, J., Mao, S., Liu, J., and Feng, D. Tribochemical Effects of Some Polymers/Stainless Steel, *Wear*, 1997; 2 (10): 238-243. [doi.org/10.1016/S0043-1648\(97\)00140-3](https://doi.org/10.1016/S0043-1648(97)00140-3)
- [27] Uyanık, E. Evaluation Creep Behaviour of Acetal / POM with Finite Element Method (master's thesis). Izmir: Ege University, 2017. <https://tez.yok.gov.tr/>
- [28] Zerkin, D. Investigation of Fatigue Behavior in Outer Tie Rods in Passenger Cars (master's thesis). Izmir: Dokuz Eylül University, 2019. <https://tez.yok.gov.tr/>

- [29] Dinc, N. Experimental and Numerical Fatigue Behaviour Analysis of a Plastically Deformed Passenger Car Tie Rod (master's thesis). Izmir: Ege University, 2017. <https://tez.yok.gov.tr/>
- [30] Chen H, Yang Y, Zhang R. Study on Electric Power Steering System Based on ADAMS. *Procedia Engineering*. Elsevier; 2011: 15: 474 - 478. [doi.org/10.1016/j.proeng.2011.08.090](https://doi.org/10.1016/j.proeng.2011.08.090)





## Appendices

# Appendix A

## Measurement Results of the Groups

Red marked values show unacceptable results.

Table A.1: Group 1 Variant 1 Measurement Results

Sample No	S <sub>ax</sub> [mm]	C <sub>min,ax</sub> [kN/mm]	M <sub>k</sub> [Nm]	Sample No	S <sub>ax</sub> [mm]	C <sub>min,ax</sub> [kN/mm]	M <sub>k</sub> [Nm]
26.1.*	0,03	188	2,3	26.1.*	0,04	169	2,7
26.1.*	0,07	155	2,7	26.1.*	0,04	185	3,1
26.1.*	0,05	182	3,1	26.1.*	0,07	168	2,5
26.1.*	0,08	180	2,3	26.1.*	0,07	153	2,6
26.1.*	0,03	180	2,7	26.1.*	0,04	210	2,6
26.1.*	0,03	220	2,7	26.1.*	0,02	152	2,8

Table A.2: Group 1 Variant 2 Measurement Results

Sample No	S <sub>ax</sub> [mm]	C <sub>min,ax</sub> [kN/mm]	M <sub>k</sub> [Nm]	Sample No	S <sub>ax</sub> [mm]	C <sub>min,ax</sub> [kN/mm]	M <sub>k</sub> [Nm]
26.1.*	0,03	205	3,5	26.1.*	0,06	173	2,6
26.1.*	0,06	173	3,1	26.1.*	0,03	240	3,2
26.1.*	0,04	230	2,9	26.1.*	0,03	203	2,6
26.1.*	0,06	216	2,7	26.1.*	0,03	170	3,0
26.1.*	0,07	201	2,5	26.1.*	0,03	208	2,9
26.1.*	0,04	206	3,4	26.1.*	0,02	177	3,1

Table A.3: Group 1 Variant 3 Measurement Results

Sample No	S <sub>ax</sub> [mm]	C <sub>min,ax</sub> [kN/mm]	M <sub>k</sub> [Nm]	Sample No	S <sub>ax</sub> [mm]	C <sub>min,ax</sub> [kN/mm]	M <sub>k</sub> [Nm]
26.1.*	0,02	229	3,9	26.1.*	0,03	192	3,4
26.1.*	0,03	197	3,5	26.1.*	0,03	201	3,6
26.1.*	0,02	264	3,3	26.1.*	0,02	240	3,2
26.1.*	0,02	229	2,8	26.1.*	0,02	233	2,9
26.1.*	0,02	230	3,8	26.1.*	0,02	230	3,4
26.1.*	0,02	269	3,7	26.1.*	0,03	192	3

Table A.4: Group 1 Variant 4 Measurement Results

Sample No	S <sub>ax</sub> [mm]	C <sub>min,ax</sub> [kN/mm]	M <sub>k</sub> [Nm]	Sample No	S <sub>ax</sub> [mm]	C <sub>min,ax</sub> [kN/mm]	M <sub>k</sub> [Nm]
26.1.*	0,02	213	3,2	26.1.*	0,01	271	3,5
26.1.*	0,01	212	3,7	26.1.*	0,01	300	3,6
26.1.*	0,01	251	3,8	26.1.*	0,01	228	3,8
26.1.*	0,02	250	3,0	26.1.*	0,02	262	3,2
26.1.*	0,01	252	4,3	26.1.*	0,01	224	3,9
26.1.*	0,01	298	4,0	26.1.*	0,01	255	4,1

Table A.5: Group 2 Variant 1 Measurement Results

Sample No	S <sub>ax</sub> [mm]	C <sub>min,ax</sub> [kN/mm]	M <sub>k</sub> [Nm]	Sample No	S <sub>ax</sub> [mm]	C <sub>min,ax</sub> [kN/mm]	M <sub>k</sub> [Nm]
26.2.*	0,03	161	3,1	26.2.*	0,03	168	2,9
26.2.*	0,06	179	2,7	26.2.*	0,03	168	3,2
26.2.*	0,03	172	3,2	26.2.*	0,03	159	2,8
26.2.*	0,02	163	2,7	26.2.*	0,07	135	2,5
26.2.*	0,03	176	3,2	26.2.*	0,03	149	2,6
26.2.*	0,03	186	3,0	26.2.*	0,03	155	3,2

Table A.6: Group 2 Variant 2 Measurement Results

Sample No	S <sub>ax</sub> [mm]	C <sub>min,ax</sub> [kN/mm]	M <sub>k</sub> [Nm]	Sample No	S <sub>ax</sub> [mm]	C <sub>min,ax</sub> [kN/mm]	M <sub>k</sub> [Nm]
26.2.*	0,03	178	3,0	26.2.*	0,03	163	3,3
26.2.*	0,03	185	3,3	26.2.*	0,03	168	2,9
26.2.*	0,03	197	3,1	26.2.*	0,02	189	3,0
26.2.*	0,03	178	3,3	26.2.*	0,03	181	3,3
26.2.*	0,02	172	2,9	26.2.*	0,06	157	2,7
26.2.*	0,07	143	2,5	26.2.*	0,03	170	3,3

Table A.7: Group 2 Variant 3 Measurement Results

Sample No	S <sub>ax</sub> [mm]	C <sub>min,ax</sub> [kN/mm]	M <sub>k</sub> [Nm]	Sample No	S <sub>ax</sub> [mm]	C <sub>min,ax</sub> [kN/mm]	M <sub>k</sub> [Nm]
26.2.*	0,03	172	3,5	26.2.*	0,03	187	3,5
26.2.*	0,03	150	3,1	26.2.*	0,03	191	3,5
26.2.*	0,03	165	3,1	26.2.*	0,03	177	3,1
26.2.*	0,02	181	3,0	26.2.*	0,03	195	3,5
26.2.*	0,02	199	3,2	26.2.*	0,03	207	3,3
26.2.*	0,03	187	3,2	26.2.*	0,03	179	3,5

Table A.8: Group 2 Variant 4 Measurement Results

Sample No	S <sub>ax</sub> [mm]	C <sub>min,ax</sub> [kN/mm]	M <sub>k</sub> [Nm]	Sample No	S <sub>ax</sub> [mm]	C <sub>min,ax</sub> [kN/mm]	M <sub>k</sub> [Nm]
26.2.*	0,03	186	3,3	26.2.*	0,02	209	3,4
26.2.*	0,03	205	3,8	26.2.*	0,03	196	3,4
26.2.*	0,03	173	3,3	26.2.*	0,03	217	3,5
26.2.*	0,02	190	3,2	26.2.*	0,03	188	3,7
26.2.*	0,03	196	3,7	26.2.*	0,03	181	3,6
26.2.*	0,03	201	3,8	26.2.*	0,03	158	3,3

Table A.9: Group 3 Variant 1 Measurement Results

Sample No	S <sub>ax</sub> [mm]	C <sub>min,ax</sub> [kN/mm]	M <sub>k</sub> [Nm]	Sample No	S <sub>ax</sub> [mm]	C <sub>min,ax</sub> [kN/mm]	M <sub>k</sub> [Nm]
26.3.1	0,03	137	1,3	26.3.7	0,03	152	1,1
26.3.2	0,03	156	0,8	26.3.8	0,03	183	1,1
26.3.3	0,03	201	1,2	26.3.9	0,03	156	1
26.3.4	0,03	167	0,9	26.3.10	0,03	171	1,1
26.3.5	0,03	195	1,1	26.3.11	0,03	171	1,2
26.3.6	0,02	225	1,2	26.3.12	0,03	187	1,4

Table A.10: Group 3 Variant 2 Measurement Results

Sample No	S <sub>ax</sub> [mm]	C <sub>min,ax</sub> [kN/mm]	M <sub>k</sub> [Nm]	Sample No	S <sub>ax</sub> [mm]	C <sub>min,ax</sub> [kN/mm]	M <sub>k</sub> [Nm]
26.3.*	0,03	180	1,2	26.3.*	0,02	230	1,4
26.3.*	0,03	208	1,3	26.3.*	0,03	225	1,2
26.3.*	0,03	195	1,4	26.3.*	0,03	192	1,0
26.3.*	0,02	210	1,6	26.3.*	0,03	180	0,9
26.3.*	0,02	158	1,5	26.3.*	0,03	195	1,3
26.3.*	0,02	250	1,4	26.3.*	0,03	178	1,3

Table A.11: Group 3 Variant 3 Measurement Results

Sample No	S <sub>ax</sub> [mm]	C <sub>min,ax</sub> [kN/mm]	M <sub>k</sub> [Nm]	Sample No	S <sub>ax</sub> [mm]	C <sub>min,ax</sub> [kN/mm]	M <sub>k</sub> [Nm]
26.4.*	0,02	273	2,1	26.4.*	0,02	242	2,4
26.4.*	0,02	235	2,2	26.4.*	0,02	253	1,8
26.4.*	0,02	235	2,1	26.4.*	0,02	267	2
26.4.*	0,02	276	2	26.4.*	0,02	242	2,3
26.4.*	0,02	293	2,1	26.4.*	0,02	222	2
26.4.*	0,02	228	1,9	26.4.*	0,02	250	2,3

Table A.12: Group 3 Variant 4 Measurement Results

Sample No	S <sub>ax</sub> [mm]	C <sub>min,ax</sub> [kN/mm]	M <sub>k</sub> [Nm]	Sample No	S <sub>ax</sub> [mm]	C <sub>min,ax</sub> [kN/mm]	M <sub>k</sub> [Nm]
26.4.*	0,01	301	3,2	26.4.*	0,02	265	3,2
26.4.*	0,01	260	3,4	26.4.*	0,02	299	2,8
26.4.*	0,01	342	3,2	26.4.*	0,02	259	2,8
26.4.*	0,01	288	3,6	26.4.*	0,01	286	3,5
26.4.*	0,01	277	3,7	26.4.*	0,02	265	2,9
26.4.*	0,02	320	3,2	26.4.*	0,02	300	3,1



# Appendix B

## Publications from the Thesis

### Conference Papers

1. Dayi S., Cevik M., Design and production of a new smaller diameter axial bearing subjected to high wear loads, 5th International Student Science Congress – İzmir Kâtip Çelebi University, 2021

# Curriculum Vitae

Name Surname : Sinan Dayı

E-mail (1) :

E-mail (2) :

## Education:

2004–2008 Niğde University, Dept. of Mechanical Engineering

2018–2021 İzmir Kâtip Çelebi University, Dept. of Mechanical Engineering

## Work Experience:

2011 – ZF Lemförder Aks Modülleri San. ve Tic. A.Ş.